CHAPTER

SUPERGEOMAGNETIC STORMS: PAST, PRESENT, AND FUTURE

7

Gurbax S. Lakhina, Bruce T. Tsurutani

Indian Institute of Geomagnetism, Navi Mumbai, India California Institute of Technology, Pasadena, CA, United States

CHAPTER OUTLINE

1 HISTORICAL BACKGROUND

A new branch of science, *geomagnetism*, came into existence in AD 1600 after the publication of *De Magnete* by William Gilbert (Gilbert, 1600). Geomagnetism was thought to have great potential for ship navigation at the time. Edmund Halley prepared the first map of the Earth's magnetic field declination by the beginning of the 18th century (Cook, 1998). The daily or diurnal variations of magnetic declination were discovered by George Graham in 1722 (Graham, 1724a,b). In 1741, large magnetic declination perturbations were observed simultaneously in London (by George Graham) and in Uppsala (by Andreas Celsius). Celsius related large magnetic declination perturbations and auroral displays over Uppsala, Sweden (Stern, 2002). The credit for discovering the phenomenon of magnetic storms goes to Alexander von Humboldt of Germany. He was working on a project to record the local magnetic declination in Berlin, each night starting from midnight to morning at intervals of

Extreme Events in Geospace. https://doi.org/10.1016/B978-0-12-812700-1.00007-8

half an hour, from May 1806 until June 1807. On the night of December 21, 1806, von Humboldt observed strong magnetic deflections for six consecutive hours in conjunction with the overhead display of northern lights (aurora borealis). He noticed that when the aurora disappeared at dawn, so did the magnetic fluctuations. Von Humboldt had the acute insight to conclude from these observations that the magnetic disturbances on the ground and the auroras in the polar sky were associated with the same phenomenon. He called this phenomenon "Magnetische Ungewitter" or a magnetic storm (von Humboldt, 1808). Many years later, it was confirmed that such "magnetic storms" were indeed a worldwide phenomena by the observations from the worldwide network of magnetic observatories (Schröder, 1997).

Research on geomagnetic activity and solar activity (sunspot observations) was conducted independently in the beginning of the 19th century. An amateur German astronomer, S. Heinrich Schwabe, began observations of sunspots in 1826. In 1843 Schwabe reported a ~10 year periodic variation of sunspots (Schwabe, 1843). Johann von Lamont reported a ~10 year periodicity in the daily variation of magnetic declination at the Munich Observatory in 1851, but he did not relate it to the sunspot cycle (Lamont, 1867; Schröder, 1997). Edward Sabine, based on the data from the wordwide network of magnetic observatories (Sabine, 1851, 1852), was the first to realize that geomagnetic activity paralleled the then recently discovered sunspot cycle. Thus, a connection between geomagnetic activity and sunspots was established.

On the morning of September 1, 1859, Richard Carrington was observing a large group of sunspots (which we now call an active region, or AR). He was extremely surprised when he saw the sudden appearance of "two brilliant beads of blinding white light" over the sunspots. The intensity of the beads increased with time for a short while and then diminished, and finally the beads disappeared (Carrington, 1859). The whole sequence lasted ~5 min. This is now considered to be the first well-documented observation of a white light (visible) solar flare on record. Richard Carrington was not the only one to record that solar flare, as it was also observed by Richard Hodgson (Hodgson, 1859) from his observatory (also in London). The two observers published simultaneously, giving confirmation of the event. However, the 1859 flare became known as the Carrington flare in recent times. On the very next day, a severe geomagnetic storm was recorded by observatories worldwide, particularly the Kew observatory and the Colaba, Bombay, observatory. Carrington was aware of this fact as he had carefully noted the occurrence of the magnetic storm, but he avoided connecting it with the solar flare. He wrote "one swallow does not make a summer" (Carrington, 1859). William Thomson, later Lord Kelvin, was convinced that there was no connection between solar and geomagnetic activities. In 1863, he showed that the Sun as a magnet was incapable of causing magnetic storms from a direct interaction. During his presidential address to the Royal Society in 1892, he stated, "It seems as if we may also be forced to conclude that the supposed connection between magnetic storms and sunspots is unreal, and that the seeming agreement between periods has been mere coincidence" (Kelvin, 1892). From his exhaustive study of sunspots, Walter Maunder demonstrated a clear latitude drift of sunspots during the sunspot cycle with a well-known butterfly diagram (Maunder, 1904a). He also proved a correlation between geomagnetic disturbances and significant developing sunspots on the surface of the sun (Maunder, 1904b,c, 1905). Whereas Maunder's conclusions about the heliolatitude drift of sunspots were more or less accepted by the astronomical community, his claim about a clear relationship between the sunspots and magnetic storms was bitterly criticized by Chree (1905) and others during the meeting report of the Royal Astronomical Society (1905) (http://adsabs.harvard.edu/abs/1905Obs%E2%80%A6.28%E2%80%A677). Association between large solar flares (arising from active sunspot regions) and magnetic storms was finally established only when sufficient statistics were gathered (Hale, 1931; Chapman and Bartels, 1940; Newton, 1943).

The advent of the space era has provided a tremendous impetus in the study of solar-terrestrial relationships. This has led to an explosion in understanding of geomagnetic storms and their solar and interplanetary causes. As a result, *space weather,* a new branch of space science, has come into existence. Essentially, space weather refers to conditions in the Sun-Earth system that can influence the performance and reliability of space-borne and ground-based technological systems and can endanger human life or health.

Geomagnetic storms are considered to be one of the most important components of space weather. During geomagnetic storms, energy is effectively transferred from the solar wind into the Earth magnetosphere, causing energization of the ring current and radiation belts, intense particle precipitation into the ionosphere, occurrence of large magnetospheric substorms, and formation of giant current loops flowing between magnetosphere and ionosphere. These effects are directly related to many technological impacts, including life-threatening power outages, satellite damage, satellite communication failures, navigational problems, and loss of LEO satellites. During "extreme" geomagnetic storms, all these effects are magnified.

2 PRESENT KNOWLEDGE ABOUT GEOMAGNETIC STORMS

According to the modern definition (Rostoker et al., 1997), a geomagnetic storm is characterized by a "main phase during which the horizontal (H) component of the Earth's low-latitude magnetic fields is significantly depressed over a time span of one to a few hours followed by its recovery, which may extend over several days." It is believed that a geomagnetic storm is caused by the movement of the intensified westward ring current (consisting of $\sim$10–300 keV magnetospheric electrons and ions) closer to Earth. This produces a depression in the H component of the geomagnetic field or the main phase of the geomagnetic storm. The recovery phase of the geomagnetic storm begins when the ring current starts to decay. The physical process of the loss of energetic particles is: charge exchange, Coulomb collisions, wave-particle interactions, and ring current energetic particle convection out of the magnetosphere (magnetopause shadowing) (Kozyra and Liemohn, 2003). The intensity of a geomagnetic storm is measured by the Dst index or by the SYM-H index. Both indices measure the symmetric ring current intensity (Iyemori, 1990). Whereas the Dst is an hourly index expressing the intensity of the ring current, the SYM-H index is the same, but computed at a 1-min time cadence (see Lakhina and Tsurutani, 2016). During magnetic storms, auroral activity intensifies and the region of auroral activity expands. Consequently, the auroras are no longer confined to the auroral oval (60–70 degrees). Auroras during magnetic storm main phases can be observed at subauroral to mid-latitudes regions.

2.1 INTERPLANETARY CAUSES OF INTENSE MAGNETIC STORMS

The main mechanism of energy transfer from the solar wind to the Earth's magnetosphere is magnetic reconnection (Dungey, 1961). Fig. 1 shows a schematic of the magnetic reconnection process. The Sun is shown on the left side and the Earth's magnetosphere on the right side of Fig. 1. The interplanetary magnetic field (IMF) carried by the solar ejecta (ICME, for example) is shown in the middle of Fig. 1. The IMF is directed southward which is opposite to the dayside magnetospheric magnetic field, a

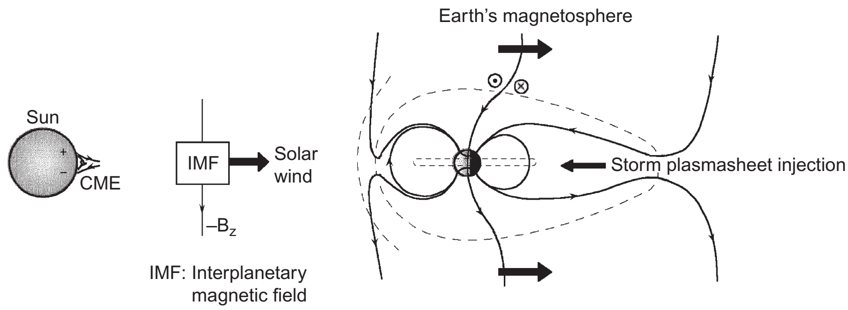

FIG. 1

A schematic of the magnetic reconnection process for the case of oppositely directed IMF and dayside Earth's magnetosphere. The magnetic reconnection subsequently leads to injection of plasma in the nightside magnetosphere.

From Tsurutani, B.T., Gonzalez, W.D., Lakhina, G.S., Alex, S., 2003. The extreme magnetic storm of 1–2 September 1859, J. Geophys. Res. 108(A7), 1268. doi:10.1029/2002JA009504.

situation most favorable for the magnetic reconnection process to operate. As a result of reconnection, the magnetic field lines on the dayside magnetosphere are eroded, and are transported to the nightside magnetotail region. Such accumulation of the magnetic field lines in the nightside magnetotail region in turn drives magnetic reconnection in the nightside magnetotail. This causes near-midnight plasma injection that leads to the excitation of auroras at high-latitude nightside regions. The energetic protons and electrons of the injected plasma drift to the west and to the east, respectively, forming a ring of current around the Earth. This "ring current" is responsible for producing a depression in the H component of the Earth's magnetic field recorded at near-equatorial observatories. It is found that the decrease in the equatorial magnetic field strength is directly proportional to the total energy of the ring current particles and, thus, could be used as a proxy for the energetics of the magnetic storm (Dessler and Parker, 1959; Sckopke, 1966; Carovillano and Siscoe, 1973).

Solar phenomena (flares, coronal holes) and related interplanetary phenomena (coronal mass ejections or ICMEs and co-rotating interaction regions or CIRs), can directly drive geomagnetic storms (Gonzalez et al., 1994; Tsurutani et al., 1995a,b, 2006). The main cause of intense magnetic storms is long duration (hours) southward IMFs (Echer et al., 2008a). The southward IMFs considerably enhance the efficiency of magnetic reconnection, the process that transfers energy from solar wind to the magnetosphere (Tsurutani and Gonzalez, 1997). This causes strong plasma injection from the magnetotail towards the inner magnetosphere leading to ring current intensification.

We point out that a one-to-one relationship between the occurrence of solar flares and ICMEs does not exist. Also there is no strong association between the flare intensity and the speed and magnetic field strength of the ICME. Several authors have reported ICME-related intense ($-250\,\text{nT} < \text{Dst} < -100\,\text{nT}$) magnetic storms that are not associated with solar flares (Tsurutani et al., 1988; Tang et al., 1989; Tang and Tsurutani, 1990; Kamide and Kusano, 2015). Further, only the magnetic cloud (MC) portions of ICMEs and not their upstream sheaths can cause magnetic storms with intensities $\text{Dst} < -250\,\text{nT}$ (Tsurutani et al., 1992a,b; Echer et al., 2008b). Tsurutani et al. (1995a, b) have shown that CIRs do not appear capable of causing such intense storms.

However, it is found that *large* solar flares (energies $\sim 10^{24}$–10^{25} J) always occur together with CME releases (Burlaga et al., 1981; Klein and Burlaga, 1982). This is because magnetic reconnection at the Sun is responsible for both phenomena at these intense levels (Shibata et al., 1995; Magara et al., 1995; Benz, 2008; Chen, 2011; Shibata and Magara, 2011). Only such intense CMEs/flares are relevant for the supermagnetic storms (Dst < -500 nT) considered in this paper.

2.2 MAGNETIC STORMS: CATEGORIES AND TYPES

Magnetic storms can be grouped into two categories as shown in Fig. 2. *Sudden impulse* (SI^+) storms are characterized by a sudden increase in the horizontal magnetic field intensity shortly before the main phase (see top panel of Fig. 2). These storms are typically caused by fast ICMEs (a requirement for producing an upstream shock). The impact of the interplanetary shock ahead of the ICME compresses the magnetosphere leading to a sudden increase in magnetic field strength, called a sudden impulse. The period between the SI^+ and the onset of the storm main phase is called the *initial phase*. However, all magnetic storms do not have initial phases. Geomagnetic storms that do not have an SI^+ are called *gradual geomagnetic* (SG) *storms* (bottom panel of Fig. 2).

Each category of storms is further classified into two types depending upon how the main phase is achieved. In single-step or Type 1 storms, the main phase occurs in one step as shown in the top panel of Fig. 3. Here, the ring current is intensified due to the magnetotail injection of energetic particles and decays to a prestorm level in one step. However, in Type 2 or in two-step storms, the main phase undergoes a two-step growth in the ring current, that is, before the ring current has decayed to a significant prestorm level, a new major particle injection occurs, leading to further buildup of ring current and further decrease of Dst. Two-step storms are caused by the compressed southward IMF in the sheath region downstream of the ICME shocks (first main phase) followed by the southward fields of magnetic cloud (second main phase) (Tsurutani and Gonzalez, 1997; Kamide et al., 1998). In general, depending upon the solar and interplanetary conditions, multi-ring current injections can occur that can cause Type 3 (three-step) or even higher step magnetic storms (Richardson and Zhang, 2008).

2.3 SOME IMPORTANT CHARACTERISTICS OF MAGNETIC STORMS

As stated earlier, the intensity of the magnetic storm is measured by the Dst index or SYM-H index at the peak of the main phase. The magnetic storms are called weak when Dst > -50 nT, moderate when $-50 >$ Dst > -100 nT, and intense when Dst < -100 nT (Kamide et al., 1998) and superintense when Dst < -500 nT (Tsurutani et al., 2003; Lakhina et al., 2005, 2012; Lakhina and Tsurutani, 2016).

Taylor et al. (1994) have shown that SI^+ magnetic storms result from interplanetary shocks associated with ICMEs while the gradual storms are caused by fast-slow stream interfaces and CIRs.

Yokoyama and Kamide (1997) conducted a superposed epoch analysis of more than 300 storms and concluded that the southward component of the IMF plays a crucial role in both triggering the main phase and in determining the magnetic storm intensity. Interestingly, the strength of the intense magnetic storm and its main-phase duration were found to be directly proportional to the strength and duration of the IMF B_z, respectively (Vichare et al., 2005; Alex et al., 2006; Rawat et al., 2007, 2010). A high solar wind dynamic pressure, in the presence of a steady southward IMF B_z with a large magnitude, is found to enhance the ring current energy leading to a severe geomagnetic storm (Rawat et al., 2010). Yokoyama and Kamide (1997) also found that the magnetic storm intensity

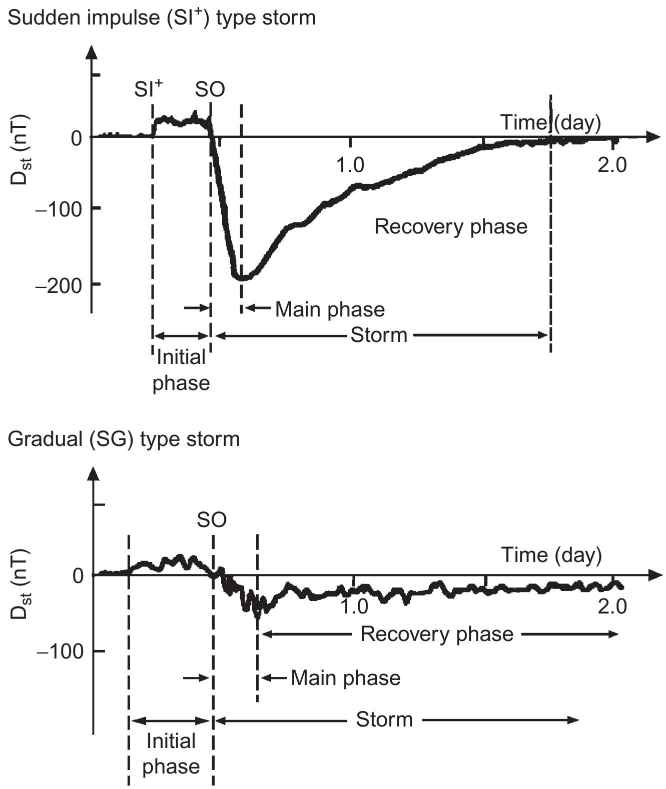

FIG. 2

Schematics of a magnetic storm: sudden impulse (SI^+) type driven by an ICME (top panel) and gradual (SG) type caused by a CIR (bottom panel). All storms may not have initial phases. The SO stands for storm onset (i.e., onset of the storm main phase).

From Tsurutani, B.T., et al., 2006. Corotating solar wind streams and recurrent geomagnetic activity: a review. J. Geophys. Res. 111, A07S01. doi:10.1029/2005JA011273; Lakhina, G.S., Alex, S., Tsurutani, B.T., Gonzalez, W.D., 2012. Super magnetic storms: hazard to society. In: Sharma, A.S., Bunde, A., Dimri, V.P., Baker, D.N. (Eds.), Extreme Events and Natural Hazards: The Complexity Perspective, Geophys. Mon. Ser., vol. 196. AGU, Washington, p. 267. doi:10.1029/2011GM001073.

depends on the duration of the main phase. The more intense storms have a longer main phase, but this relationship does not seem to apply for superintense magnetic storms.

Generally, ICME-driven storms have higher intensities (intense to superintense storm level) and shorter durations as compared to CIR-driven storms (moderate to intense storm level) intensities and durations. However, CIR-driven storms are associated with hotter plasma sheets and higher fluxes of relativistic magnetospheric electrons. Intense substorms or supersubstorms (Tsurutani et al., 2015; Hajra et al., 2016) are found to be hazardous not only to the spacecraft but also to the performance of the onboard instruments. For example, Galaxy 15 anomalies were caused by electron injection events

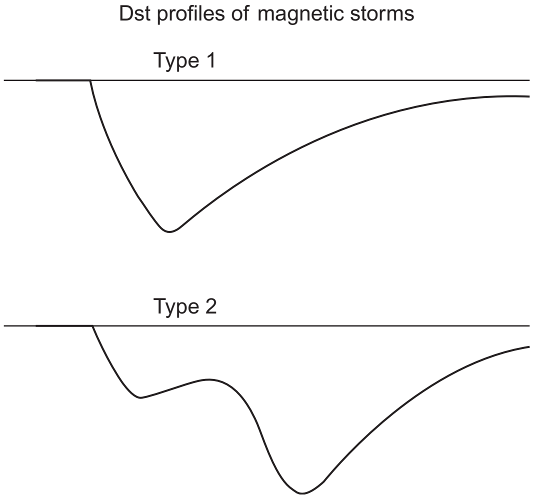

FIG. 3

Schematics of the Dst profile of Type 1 (top panel) and Type 2 (bottom panel) geomagnetic storms.

From Kamide, Y., Yokoyama, N., Gonzalez, W., Tsurutani, B., Daglis, I., Brekke, A., Masuda, S., 1998. Two-step development of geomagnetic storms. J. Geophys. Res. 103(A4), 6917–6921.

during an intense substorm (Allen, 2010). Further, the ionospheric currents due to intense substorms rather than the ring current intensity (Dst) are found to control the severity of geomagnetically induced currents (GICs) that can harm ground-based technologies, such as power grids and long pipe lines, etc. Furthermore, neither the strength of the superintense substorms nor their occurrence rate show any strong association with the intensity of the associated geomagnetic storms (Gonzalez et al., 1999; Borovsky and Denton, 2006; Kataoka and Miyoshi, 2006; Tsurutani et al., 2006, 2015; Richardson et al., 2006; Huttunen et al., 2008; Echer et al., 2008a; Allen, 2010; Yermolaev et al., 2012; Hajra et al., 2016).

Tsurutani et al. (2006) showed that the number of intense (Dst < -100 nT) storms caused by ICMEs follow the solar cycle sunspot number. However, for weak-to-moderate storms caused mainly by CIRs, there is a much smaller solar cycle dependence. The CIR-generated magnetic storms were found to have very long "recovery phases" as compared to those driven by ICMEs. The CIR "recoveries" in the high-speed streams proper can be weeks long (Tsurutani et al., 1995a,b). Further, coincident with intervals of high-speed solar wind streams, relativistic "killer" electrons suddenly appear in the outer magnetosphere during the "recovery" phase of the magnetic storms (Chapter 14 of this volume). Such energetic electrons can pose great danger for Earth-orbiting spacecraft. At present, the exact mechanism for relativistic electron acceleration in the outer magnetosphere is not known. However, there are two popular mechanisms: electron radial diffusion due to ultralow frequency (ULF) waves that break the particle's third adiabatic invariant (Hudson et al., 2000; Su et al., 2015), and energy diffusion by cyclotron-resonant interactions of electrons with a chorus that breaks their first adiabatic invariant (Summers et al., 2004; Hajra et al., 2015). For more details about the mechanisms of appearance and dropout of relativistic electrons in the radiation belts, we refer the reader to Chapter 14 of this volume.

Alex et al. (2005) and Rawat et al. (2006) found that solar energetic particle (SEP) events with high flux levels or a "plateau" after the shock passage produce much more intense storms than the events where the SEP flux levels decrease after the shock passage. Further, SEP events having longer preshock southward IMF B_z duration produced stronger main-phase storms. These results can be used as precursory signature for intense magnetic storms for space weather studies.

Tsurutani et al. (2008) studied the effects of prompt penetration electric fields (PPEFs) on the ionosphere during the great magnetic storm of October 30–31, 2003. They found that PPEFs cause the uplift of equatorial ionosphere leading to a much wider equatorial ionization anomaly in latitude. Further, the total electron content (TEC) increased from the pre-PPEF value of ~50–70 TECU to a peak value of ~270–330 TECU during the peak PPEF period.

Gonzalez et al. (2011) have studied the solar cycle and seasonal distributions of the occurrence of intense geomagnetic storms in the space era. An important result of this study is that intense storms have a dual-type distribution in the solar cycle, one at solar maximum and the second at the descending phase of the cycle, and a seasonal distribution showing the equinoctial peaks and an additional peak in July.

3 SUPERMAGNETIC STORMS

Supermagnetic storms ($Dst < -500$ nT) are relatively rare. But they are of utmost importance to society because of our ever-increasing dependence on sophisticated technology in space and on the ground. Supermagnetic storms can pose many threats: the safety of astronauts due to harmful radiation, damage to satellites, satellite communication and navigational failures, life-threatening power outages, corrosion of long pipelines due to strong geomagnetically induced currents (GICs), loss of LEO satellites, and disruption of cell phone and general communication usage (NRC Report, 2008; RAE Report, 2013; Lei et al., 2008; Thayer et al., 2008; Mannucci et al., 2005; Tsurutani et al., 2012; Lakhina et al., 2012). It is, therefore, crucial to have knowledge about the causes and occurrence of supermagnetic storms such as Carrington-type events in order to assess their potential for damaging society (Tsurutani et al., 2003; Cliver and Svalgaard, 2004; Vasyliunas, 2011; Lakhina et al., 2012; Hapgood, 2012; Riley, 2012; Cliver and Dietrich, 2013; Cid et al., 2014).

Table 1 gives a partial list of intense and superintense storms based on the magnetic field data from the Colaba and Alibag Observatories (Lakhina et al., 2012). It is noted that within the space era (since 1958), only one true supermagnetic storm has occurred. It happened on March 13–14, 1989, and had an intensity of $Dst = -589$ nT (SYM-H $= -710$ nT). The Canadian Hydro-Quebec power system was damaged due to the intense ionospheric currents during this storm (Allen et al., 1989; Bolduc, 2002). Another very intense magnetic storm, reaching almost the level of a superstorm with $Dst < -490$ nT, occurred on November 20, 2003. Only these two events can qualify as possible superstorms during the space era. Before the space age, a regularly maintained magnetic observatory network has been in existence for the past ~175 years, and many superintense storms seem to have occurred as seen from Table 1. Therefore, research on historical geomagnetic storms can extend the database of magnetic storms of superintensities (Lakhina et al., 2005, 2012).

Table 1 A List of Intense and Superintense Magnetic Storms From Colaba and Alibag Magnetic Observatories

Sr. No.	Year	Month	Day	Δ*H* (nT)	Dst (nT)	Remark
1	1847	September	24	471.3		Colaba
2	1847	October	23	534.8		Colaba
3	1848	November	17	404.0		Colaba
4	1857	December	17	306.0		Colaba
5	1859	September	1–2	1722.0		Colaba
6	1859	October	12	984.0		Colaba
7	1872	February	4	1023.0		Colaba
8	1872	October	15	430.0		Colaba
9	1882	April	17	477.0		Colaba
10	1882	November	17	445.0		Colaba
11	1882	November	19	446.0		Colaba
12	1892	February	13	612.0		Colaba
13	1892	August	12	403.0		Colaba
14	1894	July	20	525.0		Colaba
15	1894	August	10	607.0		Colaba
16	1903	October	31	819.0		Colaba
17	1909	September	25	>1500.0		Alibag
18	1921	May	13–16	>700.0		Alibag
19	1928	July	7	779.0		Alibag
20	1935	June	9	452.0		Alibag
21	1938	April	16	532.0		Alibag
22	1944	December	16	424.0		Alibag
23	1957	January	21	420.0	−250	Alibag
24	1957	September	4–5	419.0	−324	Alibag
25	1957	September	13	582.0	−427	Alibag
26	1957	September	29	483.0	−246	Alibag
27	1958	February	11	660.0	−426	Alibag
28	1958	July	8	610.0	−330	Alibag
29	1960	April	1	625.0	−327	Alibag
30	1972	June	18	230.0	−190	Alibag
31	1972	August	9	218.0	−154	Alibag
32	1972	November	1	268.0	−199	Alibag
33	1980	December	19	479.0	−240	Alibag
36	1981	March	5	406.0	−215	Alibag
35	1981	July	25	367.0	−226	Alibag
37	1982	July	13–14	410.0	−325	Alibag
38	1982	September	5–6	434.0	−289	Alibag
39	1986	February	9	342.0	−307	Alibag
40	1989	March	13	Loss	−589	Alibag

Continued

Table 1 A List of Intense and Superintense Magnetic Storms From Colaba and Alibag Magnetic Observatories—cont'd

Sr. No.	Year	Month	Day	Δ*H* (nT)	Dst (nT)	Remark
41	1989	November	17	425.0	−266	Alibag
42	1991	March	24	Loss	−298	Alibag
43	1992	February	9	225.0	−201	Alibag
44	1992	February	21	304.0	−171	Alibag
45	1992	May	10	503.0	−288	Alibag
46	1998	September	25	300.0	−207	Alibag
47	2000	April	6	384.0	−288	Alibag
48	2000	July	15	407.0	−301	Alibag
49	2001	March	31	480.0	−358	Alibag
50	2001	April	11	332.0	−256	Alibag
51	2001	November	6	359.0	−277	Alibag
52	2001	November	24	455.0	−213	Alibag
53	2003	August	18	254.0	−168	Alibag
54	2003	October	29	441.0	−345	Alibag
55	2003	October	30	506.0	−401	Alibag
56	2003	November	20	749.0	−472	Alibag
57	2004	July	27	342.0	−182	Alibag
58	2004	November	8	459.0	−383	Alibag
59	2005	May	15	352.0	−263	Alibag
60	2005	August	24	457.0	−216	Alibag

From Lakhina, G.S., Alex, S., Tsurutani, B.T., Gonzalez, W.D., 2012 Super magnetic storms: hazard to society. In: Sharma, A.S., Bunde, A., Dimri, V.P., Baker, D.N. (Eds.), Extreme Events and Natural Hazards: The Complexity Perspective, Geophys. Mon. Ser., vol. 196. AGU, Washington, p. 267. doi:10.1029/2011GM001073.

3.1 PAST SUPERMAGNETIC STORMS

One can note from Table 1 that several historical geomagnetic storms might have been of superintensities. The magnetic storms of September 1–2, 1859, (Carrington event) and February 4, 1872, have attracted great attention because of the unusual auroral sighting at low latitudes, electrical shocks and fires caused by arcing from currents induced in telegraph wires in Europe and the United States, and the disruption of telegraph communications at that time. Modern-day knowledge about the interplanetary and solar causes of the magnetic storms, and the older observations of the auroras and other effects attributed to magnetic storms, can be used to analyze historic magnetograms to deduce the possible causes of historic magnetic storms and their intensities. This approach has been applied successfully for the Carrington storm (Tsurutani et al., 2003; Lakhina et al., 2005, 2012; Lakhina and Tsurutani, 2016) and for the February 4, 1872, and other storms where interplanetary data is not available, such as March 13–14, 1989, by Lakhina and Tsurutani (2016). Here we will recapitulate some main points concerning the Carrington storm, which we believe to be the most intense magnetic storm (Dst = −1760 nT) in recorded history.

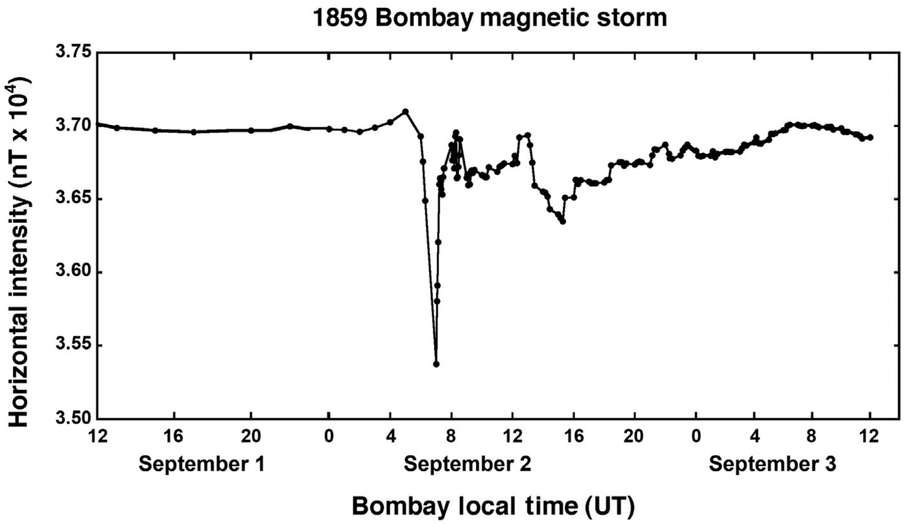

FIG. 4

The Colaba (Bombay) magnetogram for the September 1–2, 1859 magnetic storm.

From Tsurutani, B.T., Gonzalez, W.D., Lakhina, G.S., Alex, S., 2003. The extreme magnetic storm of 1–2 September 1859. J. Geophys. Res. 108(A7), 1268. doi:10.1029/2002JA009504.

Tsurutani et al. (2003) reduced the Colaba Observatory (Mumbai, India) ground magnetometer data of September 1–3, 1859. The auroral reports based on newspapers and personal correspondences with Sydney Chapman (Kimball, 1960; Loomis, 1861), and recently obtained space-age knowledge of interplanetary causes of intense storms were applied to determine the probable causes of this supermagnetic storm event. Here, we will briefly review the main characteristics of this storm (Tsurutani et al., 2003; Lakhina et al., 2005, 2012).

Fig. 4 shows the horizontal component magnetogram of September 1–3, 1859, as deduced from the Colaba Observatory (Mumbai, India) recordings by Tsurutani et al. (2003). The amplitude of the SI^+ preceding the magnetic storm is ~+120 nT. The maximum depression of the H-component at the peak of the storm main phase is $\Delta H \approx -1600$ nT. The duration of the main phase of the storm is ~1.5 h. Auroral observations (Kimball, 1960; Loomis, 1861) were used to deduce the position of the plasmapause to be at $L = 1.3$. From this information, the magnetospheric convection electric field was determined to be $E_c \sim 20$ mV m^{-1}. Assuming a 10% magnetic reconnection efficiency (Gonzalez et al., 1989), the interplanetary solar wind electric field was estimated to be $E \sim 200$ mV m^{-1}.

Considering the transit time of the ICME from the Sun to the Earth of ~17 h and 40 min (Carrington, 1859), the average shock transit speed is found to be $V_{\text{shock}} = 2380$ km s^{-1}. The relationship, $V_{\text{sw}} = 0.775\ V_{\text{shock}}$, between the solar wind speed, V_{sw}, at 1 AU and the average shock transit speed derived by Cliver et al. (1990), gives solar wind speed V_{sw} ~1850 km s^{-1} at 1 AU. Then, the relationship, B (nT) = 0.047 V_{sw} (km s^{-1}), between the V_{sw} and magnetic field B of the ejecta (Gonzalez et al., 1998) predicts the magnetic cloud magnetic field magnitude B to be ~90 nT at 1 AU. Therefore, the maximum possible interplanetary electric field for this ICME can be E ~160 mV m^{-1}. Incidentally, this value of the interplanetary electric field compares well with the above estimate based on auroral location and reconnection efficiency ($E \sim 200$ mV m^{-1}). The peak intensity of this superintense storm was estimated to be Dst = −1760 nT by assuming the ring current decay time of 1.5 h (same as the main-phase duration) and using the empirical relation for the evolution of the ring current (Burton et al., 1975). This value of the peak intensity is consistent with the Colaba local measurement of $\Delta H = -1600$ nT. Analyzing the profile of the Colaba magnetogram and by a process of elimination, Tsurutani et al. (2003) deduced that the most likely mechanism for this intense, short-duration superstorm would be a magnetic cloud with intense southward magnetic fields. It has been proposed that the second and third depressions in Dst in Fig. 4 were probably caused by the new ring current injections from the successive ICMEs near the end of the fast-recovery phase of the main (Carrington) storm, thus prolonging the overall "recovery" of the complex storm (Lakhina et al., 2012; Lakhina and Tsurutani, 2016).

Based on computer simulations, Li et al. (2006) have suggested that a high-density plasma plug could reproduce such a short time scale for the Carrington storm event with a very fast recovery after the main phase of the storm (Cid et al., 2014). Although the exact nature of this plasma plug has not been specified, it could be the high plasma density solar filaments (the most sunward part of CMEs) that are shown to play prominent roles in extreme ICME events (Kozyra et al., 2013). More detailed research and simulations are needed to test this hypothesis or to identify another possible explanation.

We point out that there is some disagreement on the minimum value of the Dst = −1760 nT for the Carrington storm in the literature. The earliest estimate for the Dst minimum for this storm was Dst = −2000 nT by Siscoe (1979) which has been revised to Dst = −850 nT by Siscoe et al. (2006). Their revised estimate is based on the assumption that taking hourly averages of the Colaba magnetogram can act as a proxy for Dst. This yielded the maximum H excursion of −859 nT instead of −1600 nT as in the unaveraged magnetogram. Siscoe et al. (2006) claim that the ICME sheath caused ∼−1600 nT depression in H seen in the Colaba magnetogram. Furthermore, some authors have raised the issue that the large drop in H component recorded at Colaba during the Carrington storm could have been caused mainly by field-aligned currents (Akasofu and Kamide, 2005; Cid et al., 2015). In our opinion the above objections are not convincing (Tsurutani et al., 2005; Lakhina and Tsurutani, 2016). Firstly, it should be noted that the hourly average of the H component of the Colaba magnetogram, or any other magnetic observatory, does not represent the true Dst. The standard Dst is based on hourly observations from several magnetic observatories widely distributed in longitude rather than from a single observatory. Secondly, the estimate of minimum Dst for the Carrington magnetic storm derived by Tsurutani et al. (2003) and Lakhina et al. (2005) is based on the calculation of the interplanetary electric field by two independent methods, namely the auroral observations and from the shock transit time from the Sun to the Earth and use of relationships between interplanetary parameters (Cliver et al., 1990; Gonzalez et al., 1998). This value of the interplanetary electric field is used in the Burton relation (Burton et al., 1975) along with a ring current decay time of 1.5 h (taken from the Colaba magnetogram) to derive the minimum Dst = −1760 nT. This value is consistent with the H depression of −1600 nT in the Colaba magnetogram. Nowhere it is implied that the H depression of −1600 nT represents the Dst value of the storm. This is a single-station observation. Incidently, interplanetary sheath fields are unlikely to have caused the extraordinary H component depression of ∼1600 nT in the Colaba magnetogram as claimed by Siscoe et al. (2006). The shocks ahead of the fast ICME can compress the magnetic field to a maximum value of four times (Kennel et al., 1985) that of the quiet field. Therefore, ICME sheath fields are expected to be ~20–40 nT which are much too low to produce the required interplanetary electric fields that can cause the H depression of ~1600 nT seen in the Colaba magnetogram (Kamide et al., 1998; Tsurutani et al., 2003). Thirdly, it should be noted that the Colaba Observatory is a near-equatorial (10^0) station. Field-aligned current cannot contribute significantly to the magnetic signature at Colaba Observatory as its location is away from the equatorial electrojet influence as well as far away from auroral ionospheric current influences during supermagnetic storms (Tsurutani et al., 2005; Lakhina and Tsurutani, 2016).

3.2 SUPERMAGNETIC STORMS: PRESENT (SPACE-AGE ERA)

As previously mentioned, the March 13–14, 1989, storm is the only event in the space-age era that can qualify as a supermagnetic storm (Allen et al., 1989). Unfortunately, the solar wind data upstream of the Earth's magnetosphere during this event is not available. The ground magnetograms show that this magnetic storm was quite unusual with a long and complex main phase.

Fig. 5 shows Dst for the Hydro-Quebec event. The peak Dst value attained at the end of the main phase was −589 nT. The corresponding maximum SYM-H value was ~−710 nT (Lakhina and Tsurutani, 2016). The storm main phase lasted for ~23 h with an onset at ~0200 UT March 13 and an approximate end at ~0100 UT March 14. The superstorm started with an SI^+ at about 0128 UT on March 13 with a magnitude of about +40 nT. There was a second SI^+ at 0747 UT on the same day with a magnitude of ~+80 nT (Allen et al., 1989). The first main phase of the storm, starting from ~0230 UT to up until ~0900 UT, was probably caused by the sheath magnetic fields, and it produced a Dst of ~−150 nT. During the second main phase lasting from ~1100 to 1200 UT, there was a sharp and smooth drop of Dst to ~−250 nT. This suggests that the second storm main phase was probably caused by a magnetic cloud with a southward B_z component. The third main phase of the storm has multiple sharp Dst excursions, most likely caused by multiple magnetic cloud southward magnetic fields. The Dst attained a peak value of −589 nT at 0100 UT on March 14. The recovery phase of the storm started ~0100 UT on March 14 and lasted till 0600 UT that day.

Fortunately, the interplanetary plasma and magnetic field data and ground magnetic data were available for the Halloween (October 29–30, 2003) and November 20, 2003, near supermagnetic storms. The intense Halloween storms were caused by two fast ICMEs with speeds ~2000 km s^{-1} (Mannucci et al., 2005; Alex et al., 2006). The impact of the first ICME caused a double storm. The first main phase due to southward sheath magnetic field occurred at ~0900 UT on October 29 with peak Dst of about ~−200 nT. The second main phase was caused by the southward magnetic cloud magnetic fields. The peak Dst value of ~−350 nT was attained at ~0125 UT on October 30. The total duration of the storm main phase was ~18 h. However, before the storm "recovery" could be completed, a second ICME impacted the Earth's magnetosphere. The strong southward field within the magnetic cloud caused a new single-step storm with a peak Dst of ~−400 nT at 2315 UT on October 30 (Mannucci et al., 2005). The main phase of this storm lasted for ~5 h.

The near supermagnetic storm of November 20, 2003, was a single-step storm with peak Dst ~ −490 nT (Alex et al., 2006; Mannucci et al., 2008). An intense southward magnetic field in the magnetic cloud portion of an ICME travelling with a speed of about 1100 km s^{-1} was responsible for causing this near superintense storm. The storm main phase lasted for ~8 h.

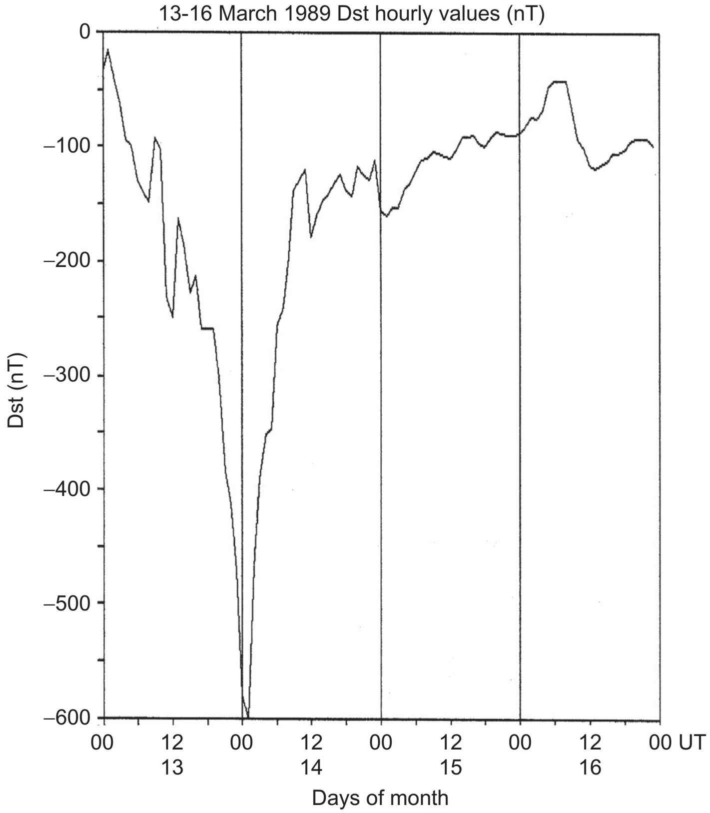

FIG. 5

Dst profile of the March 1989 supermagnetic storm from March 13–16.

From Silbergleit, V.M., Zossi de Artigas, M.M., Manzano, J.R., 1996. Austral electrojet indices derived for the great storm of March 1989. Ann. Geofis. XXXIX(6), 1177–1184.

The study of magnetic storms in the space-age era has clearly shown that the intensity of a magnetic storm depends on both the amplitudes and duration of the southward magnetic fields within the causative ICMEs.

On July 23, 2012, an extremely fast ICME with an initial speed of 2500 ± 500 km s^{-1} directed away from the Earth was observed by STEREO-A. The magnetic cloud of this ICME had an average transit speed of 1910 km s^{-1} with a peak magnetic field strength of 109 nT at 1 AU. Had this extreme ICME been directed toward Earth, it would have produced a superintense magnetic storm with Dst = – 1182 nT (Baker et al., 2013; Russell et al., 2013; Ngwira et al., 2013a,b). Liu et al. (2014) have suggested that an interaction of two successive CMEs emitted from the Sun produced such a strong magnetic cloud magnetic field.

3.3 SUPERMAGNETIC STORMS: IN FUTURE

Since modern society is becoming increasingly dependent on sophisticated space and ground technologies, future extreme events like the Carrington event can cause much more damage to society. Therefore, it is vital to know whether extreme events like the Carrington storm or even more intense storms can occur in the future. And what is the probability of occurrence of such extreme supermagnetic storms?

3.3.1 Maximum possible intensity of a supermagnetic storm

Tsurutani and Lakhina (2014) have investigated the maximum intensity of a superstorm and other related effects when a possible extreme CME hits the magnetosphere. We shall discuss the main highlights of their model. Tsurutani and Lakhina (2014) made two simple assumptions, (1) they considered the extreme value of CME speeds to be 3000 km s^{-1} near the Sun, and (2) they considered a ~10% decrease in speed (minimum drag on the ICME), or an ICME speed ~2700 km s^{-1} at 1 AU. The first assumption is justified in view of the observations of CMEs by SOHO and other spacecraft missions (Yashiro et al., 2004; Schrijver et al., 2012). The second assumption can be justified if there are multiple CME releases (and multiple flares) from the solar active regions (ARs). In such a case, the associated ICMEs tend to create a low interplanetary drag environment by "cleaning out" the upstream solar wind plasma (Tsurutani et al., 2008, 2014). Tsurutani and Lakhina (2014) employed the Rankine-Hugoniot conservation conditions to derive the shock speed (Tsurutani and Lin, 1985). Considering upstream slow solar wind speed of 350 km s^{-1}, a proton number density of 5×10^6 m^{-3}, and a downstream proton density of 20×10^6 m^{-3}, corresponding to a maximum jump of a factor of 4 in density (Kennel et al., 1985), they estimated the maximum shock speed (in Earth's reference frame) of $V_S = 3480$ km s^{-1}giving a shock transit time from the Sun to the Earth of ~12.0 h (the August 1972 event took 14.6 h and the Carrington event 17.6 h). Such a fast ICME shock will have an Alfvén Mach number of ~63 and magnetosonic Mach number of ~45. Shocks with such high Mach numbers have not been observed to date. The largest magnetosonic Mach number of the shock observed to date is ~28, and that is for the shock associated with the extreme ICME of July 23, 2012 (Riley et al., 2016).

The ram pressure downstream of the ICME shock was calculated to be 244 nPa (~240 times increase over the upstream pressure). Due to the impingement of this shock on the magnetosphere, the magnetopause will be pushed inward from its quiet time position of ~11.9 R_E to a new subsolar position at ~5.0 R_E from the center of the Earth, where R_E is an Earth radius (6371 km). So far, the lowest magnetopause position detected is at 5.2 R_E for the August 1972 storm. The magnitude of the SI^+ resulting from the magneotspheric compress was found to be $\Delta H \approx +234$ nT which exceeds the SI^+ amplitude of 202 nT recorded at Kakioka, Japan on March 24, 1991 (Araki et al., 1997).

Fast time variations in the magnetic field, of the order of dB/dt ~30 nT s^{-1}, produced by the passage of the shock through the magnetosphere, could generate a maximum magnetospheric electric field of the order of 1.9 V m^{-1}. This would produce much stronger new radiation belt fluxes in the magnetosphere, stronger than the one created on March 24, 1991 (composed of ~15 MeV electrons) when an interplanetary shock hit the Earth's magnetosphere (Blake et al., 1992; Li et al., 1993). The electric field amplitude of the March 1991 event was estimated to be ~300 mV m^{-1} (Wygant et al., 1994).

Using an empirical relationship between the speed and magnetic field strength of the ICME at 1 AU (Gonzalez et al., 1998), the magnetic cloud field strength of ~127 nT was estimated by Tsurutani and

Lakhina (2014). This yielded a maximum strength of the interplanetary electric field of ~340 mV m^{-1}, which is nearly twice the estimated value for the Carrington storm (Tsurutani et al., 2003). If we accept the fact that the intensity of all magnetic storms has a linear dependence on the interplanetary electric field (Burton et al., 1975; Echer et al., 2008b), the maximum possible intensity of a superstorm is expected to be twice the intensity of the Carrington storm, that is, Dst ≈ -3500 nT, which incidentally surpasses the maximum possible Dst limit of -2500 nT derived by Vasyliunas (2011). Vasyliunas derived this limit on the maximum Dst by setting the effective plasma pressure equal to the magnetic pressure of the dipole field at the equator of each flux tube, and applying the Dessler-Parker-Sckopke theorem. Incidently, Dst $= -31{,}000$ nT represents the absolute limit for the *H* component depression theoretically (Parker and Stewart, 1967). This could happen when the complete cancelation of the Earth's magnetic field at the equator occurs. Thus, two models independently predict that geomagnetic storms with intensities equal to or greater than that of the Carrington storm event can theoretically occur in the future.

3.3.2 Occurrence probability of carrington-type superstorms

It is not an easy task to provide a definite answer to the question "How often will a Carrington storm occur?" However, many people have made predictions, and we will briefly summarize some of those. This is discussed in more detail in Chapters 4 and 5 of this volume.

Willis et al. (1997) applied extreme value statistics to the daily *aa* indices from 1844–1993 (14 solar cycles) to find the first, second, and third largest geomagnetic storms per solar cycle. Their prediction, with a 99% probability, is that there will be no storm with $aa > 550$ for the next 100 solar cycles.

Applying extreme value theory to a Dst dataset (1957–2001), Tsubouchi and Omura (2007) predicted an occurrence frequency of a March 1989 storm (Dst $= -589$ nT) or greater intensity. Tsubouchi and Omura got a value of once in 60 years. For a Carrington-type magnetic storm (Dst $= -1760$ nT), they obtained a value of once every ~40,000 years.

Assuming that the frequency of occurrence of a storm scales as an inverse power of the intensity of the storm, Riley (2012) predicted that the probability of storms with Dst < -850 nT occurring within the next decade was ~12%. On the other hand, Love (2012) has also predicted a probability for another Carrington-type event in the next 10 years to be ~0.063. Applying lognormal statistics to the Dst time series for the years 1957–2012, Love et al. (2015) predicted that the maximum likelihood for a magnetic storm with intensity exceeding Dst < -850 nT will be about 1.13 times per century, which corresponds to approximately the same frequency as found by Riley (2012). Most recently, Riley and Love (2016) have generalized their approach, and their best estimate for the probability of a supermagnetic storm with Dst < -850 nT occurring within the next decade is $\approx 10\%$. Please see Chapter 5 of this volume for a more comprehensive analysis of these and similar methods.

Kataoka (2013) has predicted a probability of 4%–6% for a Carrington-level magnetic storm occurring during solar cycle 24. Yermolaev et al. (2013) have predicted that the occurrence frequency of a Carrington-type storm cannot exceed one event every 500 years (also please see Chapter 4 of this volume).

4 NOWCASTING AND SHORT-TERM FORECASTING OF SUPERMAGNETIC STORM

From the above discussion, it is evident that there is a large variability in the predictions of future superstorm occurrence. It is apparent that it is extremely difficult to predict when a Carrington-level supermagnetic storm will occur. For a reliable prediction of such events, we need to have either full understanding of the physical processes causing extreme ICMEs and magnetic storms or good empirical statistics of the tail of their distributions. At this stage, we do not have complete understanding of the physical processes, or have good data of the tail distributions. Therefore, we feel that at this time it is not possible to estimate the probabilities of occurrence of Carrington-level superstorms with any reasonable level of confidence.

However, in recent times, with the availability of various space missions that provide continuous monitoring of the Sun (the NASA-European Space Agency's Solar and Heliospheric Observatory (SOHO) spacecraft), and the interplanetary medium near 1 AU (e.g., NASA's Advanced Composition Explorer (ACE) spacecraft), there has been much improvement in the capability of predicting magnetic storms or space weather in real-time (nowcasting) and at a short-time scale (short-term forecasting). The nowcasting is essentially based on the use of spacecraft measurements of solar wind parameters at the Sun-Earth libration point 1 (L1 point) (Ogilvie et al., 1978; Tsurutani and Baker, 1979; Temerin and Li, 2002, 2006; Wang et al., 2003; Boynton et al., 2011; Ji et al., 2012). Two main interplanetary parameters used in most of the nowcasting or near real-time prediction schemes are the solar wind speed and the southward component of the IMF (Burton et al., 1975; Wu and Lundstedt, 1996; O'Brien and McPherron, 2000). The main advantage of nowcasting is that it has high levels of accuracy, up to 90%. However, it is limited to advance warnings of only ~0.5 h, which may not be sufficient for preventing the magnetic storm hazards.

Short-term forecasts can predict events with time scales of several hours to several days (Joselyn, 1995; Srivastava and Venkatakrishnan, 2004; Kim et al., 2005). At present, there are not any real short-term forecasting models that are operational. Instead, they are more "proof of concept" of future forecasting systems. The short-term forecasts are based essentially on the properties of CMEs and their associated shock waves, which are thought to be responsible for triggering intense and superintense magnetic storms (Gonzalez and Tsurutani, 1987; Gonzalez et al., 1994; Tsurutani et al., 1995a,b, 2006; Echer et al., 2008a,b). Since the CME parameters observed near the Sun are used, these forecasts can give a lead time of ~2–3 days. Therefore such forecasts are very practical and give sufficient time to prepare for the hazards associated with the intense magnetic storms (Brueckner et al., 1998; Gopalswamy et al., 2000; Srivastava, 2005a,b; Cho et al., 2010; Kim et al., 2014). These forecasts are also relevant for the supermagnetic storms where the lead time may be reduced to a day or less. Two main tasks for the success of the short-term forecasts are to predict the arrival time of a CME at Earth, and the magnitude of the ensuing geomagnetic storm (Gopalswamy et al., 2001; Moon et al., 2002; Cho et al., 2003; McKenna-Lawlor et al., 2006; Kim et al., 2010). Earlier models for short-term forecasts were empirical in nature using the initial speed of the ICME as an input parameter and predicting the ICME arrival at 1 AU (Gopalswamy et al., 2001). Recently, the empirical models based solely on initially observed CME parameters were extended to forecast geomagnetic storm occurrence and intensity (Dst) (Srivastava, 2005b; Kim et al., 2010). More recently, Kim et al. (2014) have developed a two-step forecast model of geomagnetic storms using CME parameters near the

Sun and solar wind conditions near 1 AU. This model's predictions have a higher success rate than the earlier models based on CME parameters alone (Gopalswamy et al., 2001; Moon et al., 2002; Cho et al., 2003; Srivastava, 2005a,b; McKenna-Lawlor et al., 2006; Kim et al., 2010). It should be noted, however, that forecasting the ICME arrival at 1 AU may be difficult when multiple CMEs are launched from an active region (Echer et al., 2009). Echer et al. (2009) surmised that complex interactions in the interplanetary medium between the Sun and Earth complicated their prediction of the arrival of the November 2004 ICMEs.

The field of nowcasting and short-term forecasting of magnetic storms is developing fast due to its application to space weather hazards (Stamper et al., 2004; Sharifi et al., 2006; Khabarova, 2007; Tsagouri et al., 2013; Love et al., 2014; Posner et al., 2014; Schrijver et al., 2015; Savani et al., 2015).

5 CONCLUSIONS

We have given an overview of the status of supermagnetic storm research. Starting from a brief historical background, we first summarized the present knowledge and then discussed its application to the analysis of past (September 1–2, 1859 Carrington event) and present (March 13–14, 1989 event) superstorms where no solar wind data was available. We then discussed the maximum possible intensity of a superstorm as well as the prediction of supermagnetic storms. Lastly, we reviewed the status of nowcasting and short-time forecasting of supermagnetic storms.

We have shown that at the present time, it is not possible to make a precise prediction of when and how often an extreme supermagnetic storm with similar or higher intensity than that of the Carrington event could occur. However, it has been theoretically shown that storms even stronger than the Carrington event can occur (provided there is corresponding extreme CME). Under ideal conditions, an extreme CME having speed of 3000 km s^{-1} near the Sun and a $\sim$10% decrease as a maximum ICME drag during its passage through the slow solar wind plasma from the Sun to 1 AU (Tsurutani and Lakhina, 2014), can excite a supermagnetic storm with intensity reaching at least the saturation value of $Dst = -2500$ nT predicted by Vasyliunas (2011). The transit time from the Sun to the Earth of an ICME shock will just be $\sim$12.0 h. The maximum amplitude of the interplanetary electric field at Earth due to this ICME will be $\sim$340 mV m^{-1}. Associated storm-time ionospheric electric fields would cause major uplift of the dayside ionosphere with substantially increased ion-neutral drag (Tsurutani et al., 2012). Supermagnetic storms of such intensity could cause havoc to modern society: loss of many low-orbiting satellites due to the additional drag, wide spread failure of telecommunications and Internet networks, failure of global positioning system (GPS) systems, and loss of navigation and power grid networks.

During the past few decades, there has been a lot of activity directed towards understanding Sun-Earth connections and space weather. Several countries—United States, Canada, Mexico, Japan, the United Kingdom, the European Union, Australia, China, South Africa—have developed their own national space weather programs based on the availability of ground-monitoring network and space missions. The ground-monitoring networks include a variety of instruments (such as magnetometers and high frequency (HF) radars) that make measurements of magnetic fields, ULF waves, total electron content using GPS systems, ionospheric irregularities, scintillations, and airglow. Space missions such as ACE, STEREO, and the deep space climate observatory (DSCOVR) are being utilized to collect interplanetary data of solar wind particles. On the other hand, solar monitoring data of flares, CMEs, X-rays and ultraviolet (UV) rays are being collected from SOHO, Hinode, GOES, DSCOVR, Solar Dynamics Observatory (SDO), etc. International programs such as International Living With the Star (ILWS), Climate and

Weather of Sun-Earth System (CAWSES), and Variability of the Sun and Its Terrestrial Impact (VarSITI) have made contributions to space weather research and prediction capabilities. As mentioned above, the nowcasting of magnetic storms has drastically improved. Short-time scale forecasting is also improving rapidly with a better understanding of the physical processes contributing to space weather. The next step is developing, testing, and validating short-time numerical space weather prediction techniques that will be able to predict space weather-related effects with the same level of accuracy as in the field of meteorology (Siscoe, 2007). Some techniques have already been developed to incorporate physics-based models, rather than just empirical models. Ideally, these types of models should cover the region from the Sun to the upper atmosphere of Earth (Tóth et al., 2007; Mannucci et al., 2015). There has been tremendous progress in developing these models in recent years and gradual improvement in prediction accuracy is expected in the coming decade.

ACKNOWLEDGMENTS

Portions of this research were conducted at the Jet Propulsion Laboratory, California Institute of Technology, under contract with NASA. GSL thanks the National Academy of Sciences, India, for support under the NASI-Senior Scientist Platinum Jubilee Fellowship. The authors thank B. I. Panchal for help in preparing Fig. 2.

GLOSSARY

Aurora A natural display of light in the polar sky. It has usually green and red optical lines, sometimes blue colors. Auroral lights are produced by the collision of energetic electrons with atoms and molecules of gases such as oxygen and nitrogen in the upper ionosphere. Auroras occur in both hemispheres in a band of latitudes called the auroral oval. The location of the auroral oval depends on the geomagnetic activity, but it usually extends from 67° to 76° magnetic latitudes. During magnetic storms, the auroral oval expands to both lower and higher magnetic latitudes. Auroras occurring in the Northern hemisphere are called the Aurora Borealis whereas those occurring in the Southern hemisphere are called the Aurora Australis.

Chorus A right-hand, circularly polarized electromagnetic planar whistler mode wave. Chorus is generated near the geomagnetic equatorial plane or in the dayside magnetospheric minimum magnetic field pockets by the loss cone instability excited by anisotropic energetic (~10–100 keV) electrons. Cyclotron resonant interaction of high-energy electrons with chorus has been proposed as a mechanism for acceleration of electrons to relativistic energies.

Coronal mass ejection (CME) A transient outflow of plasma and magnetic fields from or through the solar corona. CMEs are often, but not always, associated with disappearing solar filaments, erupting prominences, and solar flares. Large-scale closed coronal structures are a common site for CME releases. Magnetic reconnection is believed to be responsible for CMEs. The average mass and energy of the material ejected during CME can be a few times 10^{15} g and 10^{31} erg, respectively. If the magnetic field of the CME is southwardly directed, reconnection between the CME field and the Earth's field can lead to substorms and magnetic storms.

Corotating Interaction Regions (CIRs) Created when a high speed solar wind stream emanating from a coronal hole overtakes a slower (upstream) solar wind stream. The interaction leads to compression of both magnetic fields and plasma. Because coronal holes are often long lasting, the high speed streams and their interaction with slow speed streams appear to "corotate," thus the name CIR. CIRs can give rise to magnetic storms of typically weak to moderate intensity.

Dst index The "disturbance storm time" index is a measure of variations in the horizontal component of geomagnetic field due to the presence of an enhanced equatorial ring current. It is computed from magnetic data from ~4 near-equatorial stations at hourly intervals.

Geomagnetically induced currents (GICs) Induced currents produced by rapid temporal or spatial changes of magnetospheric and ionospheric currents during substorms and magnetic storms. Auroral electrojet currents with intensities of $\sim 10^6$ amperes flowing at ~100 km above the surface of the Earth can cause strong induced currents in power grid lines and pipelines. GICs can corrode long east-west extensions of pipelines and damage high-voltage power transformers.

Interplanetary coronal mass ejection (ICME): A CME is characterized by an outer loop, a dark region and a filament. The most common part of a CME detected at 1 AU from the Sun is the magnetic cloud which corresponds to the dark region of the CME. Since not all parts of a CME are detected at 1 AU, this is referred to as an Interplanetary Coronal Mass Ejection or ICME.

Magnetic declination Denotes the angle on the horizontal plane between magnetic north and geographic north. It is taken as positive when magnetic north is east of geographic north, and negative when it is to the west. Magnetic declination varies with location on the Earth's surface, and it also changes over time.

Magnetic reconnection A plasma process that converts magnetic energy to plasma kinetic energy accompanied by a change in the magnetic field topology. Magnetic reconnection prevents the excessive build-up of magnetic energy in current sheets found in space and astrophysical plasmas. It allows the transfer of magnetic flux and plasma mass between separate magnetic flux regions. Magnetic reconnection is most efficient when plasmas with oppositely directed magnetic fields are brought together. Magnetic reconnection is commonly invoked to explain the energization of plasmas and acceleration of charged particles associated with solar flares, and indirectly with magnetic storms and substorms, etc.

Ring Current Formed due to motion of trapped energetic electrons and ions (energies ~10 to ~300 keV) injected earthward from the plasma sheet in the magnetotail. The presence of magnetic field gradients and curvature forces the electrons and ions to undergo eastward and westward azimuthal drifts near the equatorial plane of the magnetosphere, respectively. These two oppositely directed drifts comprise a westward ring of current known as the Ring Current and is the main signature of a magnetic storm.

Solar flare A sudden release of energy in the solar atmosphere lasting minutes to hours, from which electromagnetic radiation (from EUV to X-ray wavelengths) and energetic charged particles are emitted. Solar flares most commonly occur at complex sunspots called active regions. Solar flares are classified according to their X-ray brightness in the wavelength range 1–8 Å. There are three categories: X-class flares are the most intense with intensities $I > 10^{-4}$ W m^{-2}, M-class flares are medium-sized with $10^{-5} \leq I < 10^{-4}$ W m^{-2}, and C-class flares are small with $10^{-6} \leq I < 10^{-5}$ W m^{-2}. Here, we denotes the peak X-ray burst intensity measured at the Earth. Each category for X-ray flares has nine subdivisions ranging from 1 to 9, e.g., X1 to X9, M1 to M9, and C1 to C9.

Substorms They occur due to injection of energetic (from 100 eV to a few tens keVs) charged particles by an explosive energy release from the near-Earth magnetotail into the nightside magnetosphere. Precipitation of these energetic charged particles into the auroral zone ionosphere produces intense auroral displays. Magnetic reconnection is believed to be responsible for the energy release. A substorm typically lasts from ~30 min to an hour.

Sunspots The dark spots on the Sun's photosphere. Sunspots appear dark as the embedded strong magnetic fields push the hot plasma out, thereby reducing the temperature compared to the surrounding area. Magnetic fields in the sunspot regions keep on evolving and become complex. Such sunspot areas are called active regions and are the potential sites for solar flares. Sunspots are the indicator of solar activity. They undergo a cyclic behavior with a period of ~11 years; this is commonly known as a *solar cycle*.

Symmetric-H (SYM-H) index Same as Dst but computed at a higher resolution of 1 min resolution instead of 1 h used for Dst.

Ultralow frequency (ULF) waves Represent a portion of the radio frequency spectrum from ~1 mHz to 30 Hz. ULF waves are produced by a variety of plasma processes occurring in the magnetosphere and the solar wind.

REFERENCES

Akasofu, S.-I., Kamide, Y., 2005. Comment on "The extreme magnetic storm of 1–2 September 1859" by B. T. Tsurutani, W. D. Gonzalez, G. S. Lakhina, and S. Alex. J. Geophys. Res. 110, https://doi.org/10.1029/2005JA011005 09226.

Alex, S., Pathan, B.M., Lakhina, G.S., 2005. Response of the low-latitude geomagnetic field to the major proton event of November 2001. Adv. Space Res. 36, 2434–2439.

Alex, S., Mukherjee, S., Lakhina, G.S., 2006. Geomagnetic signatures during the intense geomagnetic storms of 29 October and 20 November 2003. J. Atmos. Sol. Terr. Phys. 68, 769–780.

Allen, J., Sauer, H., Frank, L., Reiff, P., 1989. Effects of the March 1989 solar activity. Eos. Trans. AGU 70, 1479.

Allen, J., 2010. The Galaxy 15 anomaly: another satellite in the wrong place at a critical time. Space Weather 8. S06008. https://doi.org/10.1029/2010SW000588.

Araki, T., et al., 1997. Anomalous sudden commencement on March 24, 1991. J. Geophys. Res. 102, 14,075–14,086.

Baker, D.N., Li, X., Pulkkinen, A., Ngwira, C.M., Mays, M.L., Galvin, A.B., Simunac, K.D.C., 2013. A major solar eruptive event in July 2012: defining extreme space weather scenarios. Space Weather 11, 585–591.

Benz, A.O., 2008. Flare observations. Living Rev. Sol. Phys. 5, 1.

Blake, J.B., Kolassinski, W.A., Fillius, R.A., Mullen, E.G., 1992. Injection of electrons and protons with energies of tens of MeV into $L < 3$ onMarch 24, 1991. Geophys. Res. Lett. 19, 821–824.

Bolduc, L., 2002. GIC observations and studies in the Hydro-Quebec system. J. Atmos. Sol. Terr. Phys. 64, 1793–1802.

Borovsky, J., Denton, M.H., 2006. Differences between CME-driven storms and CIR-driven storms. J. Geophys. Res. https://doi.org/10.1029/2005JA011447.

Boynton, R.J., Balikhin, M.A., Billings, S.A., Wei, H.L., Ganushkina, N., 2011. Using the NARMAX OLS-ERR algorithm toobtain the most influential coupling functions that affect the evolution of the magnetosphere. J. Geophys. Res. 116. A05218, https://doi.org/10.1029/2010JA015505.

Brueckner, G.E., Delaboudiniere, J.-P., Howard, R.A., Paswaters, S.E., St. Cyr, O.C., Schwenn, R., Lamy, P., Simnett, G.M., Thompson, B., Wang, D., 1998. Geomagnetic storms caused by coronal mass ejections (CMEs): March 1996 through June 1997. Geophys. Res. Lett. 25, 3019–3022.

Burlaga, L.F., Sittler, E., Mariani, F., Schwenn, R., 1981. Magnetic loop behind an interplanetary shock: Voyager, Helios, and IMP 8 observations. J. Geophys. Res. 86, 6673–6684.

Burton, R.K., McPherron, R.L., Russell, C.T., 1975. An empirical relationship between interplanetary conditions and Dst. J. Geophys. Res. 80, 4204–4214.

Carovillano, R.L., Siscoe, G.L., 1973. Energy and momentum theorems in magnetospheric processes. Rev. Geophys. 11, 289.

Carrington, R.C., 1859. Description of a singular appearance seen in the Sun on September 1, 1859. Mon. Not. R. Astron. Soc. 20, 13–15.

Chapman, S., Bartels, J., 1940. Geomagnetism, vol. 1. Oxford Univ Press, New York. pp. 328–337.

Chen, P.F., 2011. Coronal mass ejections: models and their observational basis. Living Rev. Sol. Phys. 8, 1.

Cho, K.-S., Moon, Y.-J., Dryer, M., Fry, C.D., Park, Y.-D., Kim, K.-S., 2003. A statistical comparison of interplanetary shock and CME propagation models. J. Geophys. Res. 108 (A12), 1445. https://doi.org/10.1029/2003JA010029.

Cho, K.-S., Bong, S.-C., Moon, Y.-J., Dryer, M., Lee, S.-E., Kim, K.-H., 2010. An empirical relationship between coronal mass ejection initial speed and solar wind dynamic pressure. J. Geophys. Res. 115. A10111. https://doi.org/10.1029/2009JA015139.

Chree, C., 1905. Review of Maunder's recent investigations on the cause of magnetic disturbances. J. Geophys. Res. 10, 9–14. https://doi.org/10.1029/TE010i001p00009.

Cid, C., Palacios, J., Saiz, E., Guerrero, A., Cerrato, Y., 2014. On extreme geomagnetic storms. J. Space Weather Space Clim. 4, 28. https://doi.org/10.1051/swsc/2014026.

Cid, C., Saiz, E., Guerrero, A., Palacios, J., Cerrato, Y., 2015. A Carrington-like geomagnetic storm observed in the 21st century. J. Space Weather Space Clim. 5, https://doi.org/10.1051/swsc/2015017. 16.

Cliver, E., Feynman, J., Garrett, H., 1990. An estimate of the maximum speed of the solar wind, 1938–1989. J. Geophys. Res. 95 (A10), 17103–17112.

Cliver, E.W., Dietrich, W.F., 2013. The 1859 space weather event revisited: limits of extreme activity. J. Space Weather Space Clim. 3, 31. https://doi.org/10.1051/swsc/2013053.

Cliver, E.W., Svalgaard, L., 2004. The 1859 solar-terrestrial disturbance and the current limits of extreme space weather activity. Solar Phys. 224, 407–422.

Cook, A., 1998. Edmond Halley: Charting the Heavens and the Seas. Oxford University Press, Oxford. ISBN: 0198500319.

Dessler, A.J., Parker, E.N., 1959. Hydromagnetic theory of magnetic storms. J. Geophys. Res. 64, 2239.

Dungey, J.W., 1961. Interplanetary magnetic field and the auroral zones. Phys. Rev. Lett. 6, 47.

Echer, E., Gonzalez, W.D., Tsurutani, B.T., Gonzalez, A.L.C., 2008a. Interplanetary conditions causing intense geomagnetic storms ($Dst \leq \_100$ nT) during solar cycle 23 (1996–2006). J. Geophys. Res. 113. A05221. https://doi.org/10.1029/2007JA012744.

Echer, E., Gonzalez, W.D., Tsurutani, B.T., 2008b. Interplanetary conditions leading to super intense geomagnetic storms ($Dst \leq -250$ nT) during solar cycle 23. Geophys. Res. Lett. 35, 03–06. https://doi.org/10.1029/2007GL031755.

Echer, E., Tsurutani, B.T., Guarnieri, F.L., 2009. Solar and interplanetary origins of the November 2004 superstorms. Adv. Space Res. 44, 615–620.

Gilbert, W., 1600. De Magnete. Chiswick, London (English translation by P. F. Mottelay, Dover, New York, 1958.).

Gonzalez, W.D., Tsurutani, B.T., 1987. Criteria of interplanetary parameters causing intense magnetic storms ($Dst < -100$ nT). Planet. Space Sci. 35, 1101–1109.

Gonzalez, W.D., Tsurutani, B.T., Gonzalez, A.L.C., Smith, E.J., Tang, F., Akasofu, S.I., 1989. Solar wind-magnetosphere coupling during intense magnetic storms (1978–1979). J. Geophys. Res. 94 (A7), 8835–8851.

Gonzalez, W.D., Tsurutani, B.T., Clúa de Gonzalez, A.L., 1999. Interplanetary origin of geomagnetic storms. Space Sci. Rev. 88, 529–562.

Gonzalez, W., Joselyn, J., Kamide, Y., Kroehl, H., Rostoker, G., Tsurutani, B., Vasyliunas, V., 1994. What is a geomagnetic storm? J. Geophys. Res. 99 (A4), 5771–5792.

Gonzalez, W.D., de Gonzalez, A.L.C., Dal Lago, A., Tsurutani, B.T., Arballo, J.K., Lakhina, G.S., Buti, B., Ho, C.M., Wu, S.-T., 1998. Magnetic cloud field intensities and solar wind velocities. Geophys. Res. Lett. 25 (7), 963–966.

Gonzalez, W.D., Echer, E., Clade Gonzalez, A.L., Tsurutani, B.T., Lakhina, G.S., 2011. Extreme geomagnetic storms, recent Gleissberg cycles and space era super intense storms. J. Atmos. Sol. Terr. Phys. 73 (11–12), 1447–1453. https://doi.org/10.1016/j.jastp.2010.07.023.

Gopalswamy, N., Lara, A., Lepping, R.P., Kaiser, M.L., Berdichevsky, D., St. Cyr, O.C., 2000. Interplanetary acceleration of coronal mass ejections. Geophys. Res. Lett. 27, 145–148.

Gopalswamy, N., Lara, A., Yashiro, S., Kaiser, M., Howard, R.A., 2001. Predicting the 1-AU arrival times of coronal mass ejections. J. Geophys. Res. 106, 29,207–29,217.

Graham, G., 1724a. An account of observations made of the variation of the horizontal needle at London, in the latter part of the year 1722, and beginning of 1723. Philos. Trans. R. Soc. Lond. A 33, 96–107. https://doi.org/10.1098/rstl.1724.0020.

Graham, G., 1724b. Observations of the dipping needle, made at London, in the beginning of the year 1723. Philos. Trans. R. Soc. Lond. A 33, 332–339. https://doi.org/10.1098/rstl.1724.0062.

Hajra, R., Tsurutani, B.T., Echer, E., Gonzalez, W.D., Santolik, O., 2015. Relativistic (E > 0.6, > 2.0 and > 4.0 MeV) electron acceleration at geosynchronous orbit during high-intensity, long-duration, continuous AE activity (HILDCAA) events. Astrophys. J. 799, 39. https://doi.org/10.1088/0004-637X/799/1/39.

Hajra, R., Tsurutani, B.T., Echer, E., Gonzalez, W.D., Gjerloev, J.W., 2016. Supersubstorms (SML ≤ -2500 nT): magnetic storm and solar cycle dependences. J. Geophys. Res. Space Phys. 121, 7805–7816. https://doi.org/10.1002/2015JA021835.

Hale, G.E., 1931. The spectroheliscope and its work. part III. Solar eruptions and their apparent terrestrial effects. Astrophys. J. 73, 379–412.

Hapgood, M.A., 2012. Prepare for the coming space weather storm. Nature 484, 311–313. https://doi.org/10.1038/484311a.

Hodgson, R., 1859. On a curious appearance seen in the Sun. Mon. Not. R. Astron. Soc. 20, 15–16.

Hudson, M.K., Elkington, S.R., Lyon, J.G., Goodrich, C.C., 2000. Increase in relativistic electron flux in the inner magnetosphere: ULF wave mode structure. Adv. Space Res. 25, 2327–2337.

Huttunen, K.E.J., Kilpua, S.P., Pulkkinen, A., Viljanen, A., Tanskanen, E., 2008. Solar wind drivers of large geomagnetically induced currents during the solar cycle 23. Space Weather 6. S10002. https://doi.org/10.1029/2007SW000374.

Iyemori, T., 1990. Storm-time magnetospheric currents inferred from midlatitude geomagnetic field variations. J. Geomag. Geoelec. 42, 1249–1265.

Ji, E.-Y., Moon, Y.-J., Gopalswamy, N., Lee, D.-H., 2012. Comparison of Dst forecast models for intense geomagnetic storms. J. Geophys. Res. 117. A03209. https://doi.org/10.1029/2011JA016872.

Joselyn, J.A., 1995. Geomagnetic activity forecasting: the state of the art. Rev. Geophys. 33, 383.

Kamide, Y., Yokoyama, N., Gonzalez, W., Tsurutani, B., Daglis, I., Brekke, A., Masuda, S., 1998. Two-step development of geomagnetic storms. J. Geophys. Res. 103 (A4), 6917–6921.

Kamide, Y., Kusano, K., 2015. No major solar flares but the largest geomagnetic storm in the present solar cycle. Space Weather 13, 365–367. https://doi.org/10.1002/2015SW001213.

Kataoka, R., Miyoshi, Y., 2006. Flux enhancement of radiation belt electrons during geomagnetic storms driven by coronal mass ejections and corotating interaction regions. Space Weather 4. S09004. https://doi.org/10.1029/2005SW000211.

Kataoka, R., 2013. Probability of occurrence of extreme magnetic storms. Space Weather 11, 214–218. https://doi.org/10.1002/swe.20044.

Kelvin, W.T., 1892. Address to the Royal Soc. Nov. 30. Proc. R. Soc. Lond. A 52, 302–310.

Kennel, C.F., Edmiston, J.P., Hada, T., 1985. A quarter century of collisionless shock research. In: Collisionless Shocks in the Heliosphere: A Tutorial Review. Geophys. Mon. Ser., vol. 34. AGU, Washington, DC, pp. 1–36.

Khabarova, O.V., 2007. Current problems of magnetic storm prediction and possible ways of their solving. Sun Geosph. 2 (1), 32–37.

Kim, R.-S., Cho, K.-S., Moon, Y.-J., Kim, Y.-H., Yi, Y., Dryer, M., Bong, S.-C., Park, Y.-D., 2005. Forecast evaluation of the coronal mass ejection(CME) geoeffectiveness using halo CMEs from 1997 to 2003. J. Geophys. Res. 110. A11104. https://doi.org/10.1029/2005JA011218.

Kim, R.-S., Cho, K.-S., Moon, Y.-J., Dryer, M., Lee, J., Yi, Y., Kim, K.-H., Wang, H., Park, Y.-D., Kim, Y.-H., 2010. An empirical model for prediction of geomagnetic storms using initially observed CME parameters at the Sun. J. Geophys. Res. 115. A12108. https://doi.org/10.1029/2010JA015322.

Kim, R.-S., Moon, Y.-J., Gopalswamy, N., Park, Y.-D., Kim, Y.-H., 2014. Two-step forecast of geomagnetic storm using coronal mass ejection and solar wind condition. Space Weather 12, 246–256. https://doi.org/10.1002/2014SW001033.

Kimball, D.S., 1960. A Study of the Aurora of 1859. Sci. Rep. 6, UAG-R109Univ. of Alaska, Fairbanks.

Klein, L.W., Burlaga, L.F., 1982. Magnetic clouds at 1 AU. J. Geophys. Res. 87, 613.

Kozyra, J.U., Liemohn, M.W., 2003. Ring current energy input and decay. Space Sci. Rev. 109, 105–131.

Kozyra IV, J.U., Escoubet, W.B.M., Lepri, C.P., Liemohn, M.W., Gonzalez, W.D., Thomsen, M.W., Tsurutani, B.T., 2013. Earth's collision with a solar filament on 21January 2005: overview. J. Geophys. Res. 118, 5967–5978. https://doi.org/10.1002/jgra.50567.

Lakhina, G.S., Tsurutani, B.T., 2016. Geomagnetic storms: historical perspective to modern view. Geosci. Lett. 3, 5. https://doi.org/10.1186/s40562-016-0037-4.

Lakhina, G.S., Alex, S., Tsurutani, B.T., Gonzalez, W.D., 2012. Super magnetic storms: hazard to society. In: Sharma, A.S., Bunde, A., Dimri, V.P., Baker, D.N. (Eds.), Extreme Events and Natural Hazards: The Complexity Perspective. Geophys. Mon. Ser., 196, AGU, Washington. https://doi.org/10.1029/2011GM001073 p. 267.

Lakhina, G.S., Alex, S., Tsurutani, B.T., Gonzalez, W.D., 2005. Research on historical records of geomagnetic storms, in Coronal and Stellar Mass Ejections. In: Dere, K.P., Wang, J., Yan, Y. (Eds.), Proceedings of the 226th Symposium of the International Astronomical Union held in Beijing, China, September 13–17, 2004, Cambridge Univ. Press, Cambridge. UK. pp. 3–15.

Lamont, J., 1867. Handbuch des Magnetismus. Leopold Voss, Leipzig.

Lei, J., Thayer, J.P., Forbes, J.M., Wu, Q., She, C., Wan, W., Wang, W., 2008. Ionosphere response to solar wind high-speed streams. Geophys. Res. Lett. 35, 19105. https://doi.org/10.1029/2008GL035208.

Li, X.L., Roth, I., Temerin, M., Wygant, J.R., Hudson, M.K., Blake, J.B., 1993. Simulation of the prompt energization and transport of radiation belt particles during the March 24, 1991 SSC. Geophys. Res. Lett. 20, 2423–2426.

Li, X., Temerin, M., Tsurutani, B.T., Alex, S., 2006. Modeling of 1–2 September 1859 super magnetic storm. Adv. Space Res. 38, 273–279.

Liu, Y.D., Luhmann, J.G., Kajdic, P., Kilpua, E.K., Lugaz, N., et al., 2014. Observations of an extreme storm in interplanetary space caused by successive coronal mass ejections. Nat. Commun. 5, 3481.

Loomis, E., 1861. On the great auroral exhibition of Aug. 28th to Sept. 4, 1859, and on auroras generally. Am. J. Sci. 82, 318–335.

Love, J.J., 2012. Credible occurrence probabilities for extreme geophysical events: earthquakes, volcanic eruptions, magnetic storms. Geophys. Res. Lett. 39, 10301. https://doi.org/10.1029/2012GL051431.

Love, J.J., Rigler, E.J., Pulkkinen, A., Balch, C.C., 2014. Magnetic storms and induction hazards. Eos. Trans. AGU 95 (48), 445–452.

Love, J.J., Rigler, E.J., Pulkkinen, A., Riley, P., 2015. On the lognormality of historical magnetic storm intensity statistics: implications for extreme-event probabilities. Geophys. Res. Lett. 42, 6544–6553. https://doi.org/10.1002/2015GL064842.

Magara, T., Shibata, K., Yokoyama, T., 1995. Evolution of eruptive flares. I. plasmoid dynamics in eruptive flares. Astrophys. J. 487, 437–446.

Mannucci, A.J., Tsurutani, B.T., Iijima, B.A., Komjathy, A., Saito, A., Gonzalez, W.D., Guarnieri, F.L., Kozyra, J.U., Skoug, R., 2005. Dayside global ionospheric response to the major interplanetary events of October 29–30, 2003 "Halloween Storms" Geophys. Res. Lett. 32, https://doi.org/10.1029/2004GL021467. L12S02.

Mannucci, A.J., Tsurutani, B.T., Abdu, M.A., Gonzalez, W.D., Komjathy, A., Echer, E., Iijima, B.A., Crowley, G., Anderson, D., 2008. Superposed epoch analysis of the dayside ionospheric response to four intense geomagnetic storms. J. Geophys. Res. 113, 00–02. https://doi.org/10.1029/2007JA012732.

Mannucci, A.J., Verkhoglyadova, O.P., Tsurutani, B.T., Meng, X., Pi, X., Wang, C., Rosen, G., Lynch, E., Sharma, S., Ridley, A., Manchester, W., Van Der Holst, B., Echer, E., Hajra, R., 2015. Medium-range thermosphere-ionosphere storm forecasts. Space Weather 13, 125–129. https://doi.org/10.1002/2014SW001125.

Maunder, E.W., 1904a. Note on the distribution of sun-spots in the heliographic latitude, 1874 to 1902. Mon. Not. R. Astron. Soc. 64, 747–761. https://doi.org/10.1093/mnras/64.8.747.

Maunder, E.W., 1904b. Magnetic disturbances, 1882 to 1903, as recorded at the Royal Observatory Greenwich, and their association with sun-spots. Mon. Not. R. Astron. Soc. 65, 2–18. https://doi.org/10.1093/mnras/65.1.2.

Maunder, E.W., 1904c. Demonstration of the solar origin of the magnetic disturbances. Mon. Not. R. Astron. Soc. 65, 18–34. https://doi.org/10.1093/mnras/65.1.18.

Maunder, E.W., 1905. Magnetic disturbances as recorded at the Royal Observatory Greenwich, and their association with sun-spots. Mon. Not. R. Astron. Soc. 65, 538–559. https://doi.org/10.1093/mnras/65.6.538.

McKenna-Lawlor, S.M.P., Dryer, M., Kartalev, M.D., Smith, Z., Fry, C.D., Sun, W., Deehr, C.S., Kecskemety, K., Kudela, K., 2006. Near real-time predictions of the arrival at Earth of flare-related shocks during Solar Cycle 23. J. Geophys. Res. 111. A11103. https://doi.org/10.1029/2005JA011162.

Moon, Y.-J., Dryer, M., Smith, Z., Park, Y.-D., Cho, K.-S., 2002. A revised shock time of arrival (STOA) model for interplanetary shock propagation: STOA-2. Geophys. Res. Lett. 29 (10), 1390. https://doi.org/10.1029/2002GL014865.

Newton, H.W., 1943. Solar flares and magnetic storms. Mon. Not. R. Astron. Soc. 103, 244–257.

National Research Council, 2008. Severe Space Weather Events-Understanding Societal and Economic Impacts. National Academies Press, Washington, DC.

Ngwira, C.M., Pulkkinen, A., Mays, M.L., Kuznetsova, M.M., Galvin, A.B., et al., 2013a. Simulation of the 23 July 2012 extreme space weather event: what if this extremely rare cme was earth directed? Space Weather 11, 671–679.

Ngwira, C.M., Pulkkinen, A., Kuznetsova, M.M., Glocer, A., 2013b. Modeling extreme Carrington-type space weather events using three-dimensional global MHD simulations. J. Geophys. Res. 119, 4456–4474. https://doi.org/10.1002/2013JA019661.

O'Brien, T.P., McPherron, R.L., 2000. An empirical phase space analysis of ring current dynamics: Solar wind control of injection and decay. J. Geophys. Res. 105, 7707–7719.

Ogilvie, K.W., Durney, A., von Rosenvinge, T., 1978. Descriptions of experimental investigations and instruments for the ISEE spacecraft. IEEE Trans. Geosci. Electron. GE-16 (3), 151–153. https://doi.org/10.1109/TGE.1978.294535.

Parker, E.N., Stewart, H.A., 1967. Nonlinear inflation of a magnetic dipole. J. Geophys. Res. 72, 5287–5293.

Posner, A., Hesse, M., St. Cyr, O.C., 2014. The main pillar: assessment of space weather observational asset performance supporting nowcasting, forecasting, and research to operations. Space Weather 12, 257–276. https://doi.org/10.1002/2013SW001007.

Rawat, R., Alex, S., Lakhina, G.S., 2006. Low-latitude geomagnetic signatures during major solar energetic particle events of solar cycle-23. Ann. Geophys. 24, 3569–3583.

Rawat, R., Alex, S., Lakhina, G.S., 2007. Geomagnetic storm characteristics under varied interplanetary conditions. Bull. Astron. Soc. India 35, 499–509.

Rawat, R., Alex, S., Lakhina, G.S., 2010. Storm-time characteristics of intense geomagnetic storms (Dst < - 200 nT) at low-latitudes and associated energetics. J. Atmos. Sol. Terr. Phys. 72, 1364–1371. https://doi.org/10.1016/j.jastp.2010.09.029.

Richardson, I.G., et al., 2006. Major geomagnetic storms (Dst < -100 nT) generated by corotating interaction regions. J. Geophys. Res. 111, https://doi.org/10.1029/2005JA011476. A07S09.

Richardson, I.G., Zhang, J., 2008. Multiple-step geomagnetic storms and their interplanetary drivers. Geophys. Res. Lett. 35, https://doi.org/10.1029/2007GL032025 L06S07.

Riley, P., 2012. On the probability of occurrence of extreme space weather events. Space Weather 10, https://doi.org/10.1029/2011SW000734. 02012.

Riley, P., Caplan, R.M., Giacalone, J., Lario, D., Liu, Y., 2016. Properties of the fast forward shock driven by the 2012 July 23 extreme coronal mass ejection. Astrophys. J. 819, 57. https://doi.org/10.3847/0004-637X/819/1/57. (11 pp.).

Riley, P., Love, J.J., 2016. Extreme geomagnetic storms: probabilistic forecasts and their uncertainties. Space Weather 15. https://doi.org/10.1002/2016SW001470.

Rostoker, G., Friedrich, E., Dobbs, M., 1997. Physics of magnetic storms. In: Tsurutani, B.T., Gonzalez, W.D., Kamide, Y., Arballo, J.K. (Eds.), Magnetic Storms. Geophys. Monogr. Ser., 98, AGU, Washington, pp. 149–160.

Royal Academy of Engineering Report, 2013. Extreme Space Weather Impacts on Engineered Systems and Infrastructure. Royal Academy of Engineering, London.

Royal Astronomical Society, 1905. The Observatory, XXVIII, No. 354.

Russell, C.T., Mewaldt, R.A., Luhmann, J.G., Mason, G.M., von Rosenvinge, T.T., et al., 2013. The very unusual interplanetary coronal mass ejection of 2012July 23: a blast wave mediated by solar energetic particles. Astrophys. J. 770, 38.

Sabine, E., 1851. On periodical laws discoverable in mean effects on the larger magnetic disturbances. Philos. Trans. R. Soc. Lond. 141, 103–129.

Sabine, E., 1852. On periodical laws discoverable in mean effects on the larger magnetic disturbances, ii. Philos. Trans. R. Soc. Lond. A 142, 234–235.

Savani, N.P., Vourlidas, A., Szabo, A., Mays, M.L., Richardson, I.G., Thompson, B.J., Pulkkinen, A., Evans, R., Nieves-Chinchilla, T., 2015. Predicting the magnetic vectors within coronal mass ejections arriving at Earth: 1 Initial architecture. Space Weather 13, 374–385. https://doi.org/10.1002/2015SW001171.

Schrijver, C.J., Beer, J., Baltensperger, U., Cliver, E.W., Güdel, M., et al., 2012. Estimating the frequency of extremely energetic solar events, based on solar, stellar, lunar, and terrestrial records. J. Geophys. Res. 117. 08103. https://doi.org/10.1029/2012JA017706.

Schrijver, C.J., Kauristie, K., Aylward, A.D., Denardini, C.M., Gibson, S.E., Glover, A., Gopalswamy, N., Grande, M., Hapgood, M., Heynderickx, D., Jakowski, N., Kalegaev, V.V., Lapenta, G., Linker, J.A., Liu, S., Mandrini, C.H., Mann, I.R., Nagatsuma, T., Nandy, D., Obara, T., O'Brien, T.P., Onsager, T., Opgenoorth, H.J., Terkildsen, M., Valladares, C.E., Vilmer, N., 2015. Understanding space weather to shield society: a global road map for 2015–2025 commissioned by COSPAR and ILWS. Adv. Space Res. 55, 2745–2807.

Schröder, W., 1997. Some aspects of the earlier history of solar terrestrial physics. Planet. Space Sci. 45, 395–400.

Schwabe, S.H., 1843. Solar observations during 1843. Astron. Nachr. 20 (495), 234–235.

Sckopke, N., 1966. A general relation between the energy of trapped particles and the disturbance field near the Earth. J. Geophys. Res. 71, 3125.

Sharifi, J., Araabi, B.N., Lucas, C., 2006. Multi-step prediction of *Dst* index using singular spectrum analysis and locally linear neurofuzzy modeling. Earth Planets Space 58, 331–341.

Shibata, K., Masuda, S., Shimojo, M., Hara, H., Yokoyama, T., Tsuneta, S., Kosugi, T., Ogawara, Y., 1995. Hot plasma ejections associated with compact-loop solar flares. Astrophys. J. Lett. 451, 83.

Shibata, K., Magara, T., 2011. Solar flares: magnetohydrodynamic processes. Living Rev. Sol. Phys. 8, 6.

Siscoe, G.L., 1979. A quasi-self-consistent axially symmetric model for the growth of a ring current through earthward motion from a pre-storm configuration. Planet. Space Sci. 27, 285–295.

Siscoe, G., Crooker, N.U., Clauer, C.R., 2006. Dst of the Carrington storm of 1859. Adv. Space Res. 38, 173–179.

Siscoe, G., 2007. Space weather forecasting historically viewed through the lens of meteorology. In: Bothmer, V., Daglis, I. (Eds.), Space Weather, Physics and Effects. Springer, Berlin.

Srivastava, N., Venkatakrishnan, P., 2004. Solar and interplanetary sources of major geomagnetic storms during 1996–2002. J. Geophys. Res. 109. A010103. https://doi.org/10.1029/2003JA010175.

Srivastava, N., 2005a. Predicting the occurrence of super-storms. Ann. Geophys. 23, 2989–2995.

Srivastava, N., 2005b. A logistic regression model for predicting the occurrence of intense geomagnetic storms. Ann. Geophys. 23, 2969–2974.

Stamper, R., Belehaki, A., Buresova, D., Cander, L.R., Kutiev, I., Pietrella, M., Stanislawska, I., Stankov, S., Tsagouri, I., Tulunay, Y.K., Zolesi, B., 2004. Nowcasting, forecasting and warning for ionospheric propagation: tools and methods. Ann. Geophys. 47 (2/3), 957–983.

Stern, D.P., 2002. A millennium of geomagnetism. Rev. Geophys. 40 (3), 1007. https://doi.org/10.1029/2000RG000097.

Su, Z., et al., 2015. Ultra-low-frequency wave-driven diffusion of radiation belt relativistic electrons. Nat. Commun. 6, 10096. https://doi.org/10.1038/ncomms10096(2015).

Summers, D., Ma, C., Meredith, N.P., Horne, R.B., Thorne, R.M., Anderson, R.R., 2004. Modeling outer-zone relativistic electron response to whistler-mode chorus activity during substorms. J. Atmos. Sol. Terr. Phys. 66, 133.

Tang, F., Tsurutani, B.T., Gonzalez, W.D., Akasofu, S.I., Smith, E.J., 1989. Solar sources of interplanetary southward B_z events responsible for major magnetic storms (1978–1979). J. Geophys. Res. 94, 3535–3541.

Tang, F., Tsurutani, B.T., 1990. Reply. J. Geophys. Res.. 95, 10721.

Taylor, J.R., Lester, M., Yeoman, T.K., 1994. A superposed epoch analysis of geomagnetic storms. Ann. Geophys. 12, 612–624.

Temerin, M., Li, X., 2002. A new model for the prediction of Dst on the basis of the solar wind. J. Geophys. Res. 107 (A12), 1472. https://doi.org/10.1029/2001JA007532.

Temerin, M., Li, X., 2006. Dst model for 1995–2002. J. Geophys. Res. 111. A04221. https://doi.org/10.1029/2005JA011257.

Thayer, J.P., Lei, J., Forbes, J.M., Sutton, E.K., Nerem, R.S., 2008. Thermospheric density oscillations due to periodic solar wind high speed streams. J. Geophys. Res. 113. 06307. https://doi.org/10.1029/2008JA013190.

Tóth, G., Zeeuw, D.L., Gombosi, T.I., Manchester, W.B., Ridley, A.J., Sokolov, I.V., Roussev, I.I., 2007. Sunto-thermosphere simulation of the 28–30 October 2003 storm with the Space Weather Modeling Framework. Space Weather 5, S06003. https://doi.org/10.1029/2006SW000272.

Tsagouri, I., Belehaki, A., Bergeot, N., Cid, C., Delouille, V., et al., 2013. Progress in space weather modeling in an operational environment. J. Space Weather Space Clim. 3, A17.

Tsubouchi, K., Omura, Y., 2007. Long-term occurrence probabilities of intense geomagnetic storm events. Space Weather 5, 12003. https://doi.org/10.1029/2007SW000329.

Tsurutani, B.T., Baker, D.N., 1979. Substorm warnings: an ISEE-3 real time data system. Eos 60, 702.

Tsurutani, B.T., Lin, R.P., 1985. Acceleration of > 47 keV ions and > 2 keV electrons by interplanetary shocks at 1 AU. J. Geophys. Res. 90, 1.

Tsurutani, B.T., Gonzalez, W.D., Tang, F., Akasofu, S.I., Smith, E.J., 1988. Origin of interplanetary southward magnetic fields responsible for major magnetic storms near solar maximum(1978–1979). J. Geophys. Res. 93 (A8), 8519–8531.

Tsurutani, B.T., Gonzalez, W.D., Tang, F., Lee, Y.T., Okada, M., Park, D., 1992a. Reply to L. J. Lanzerotti: Solar wind RAM pressure corrections and an estimation of the efficiency of viscous interaction. Geophys. Res. Lett. 19((19), 1993–1994.

Tsurutani, B.T., Gonzalez, W.D., Tang, F., Lee, Y.T., 1992b. Great magnetic storms. Geophys. Res. Lett. 19, 73.

Tsurutani, B.T., Gonzalez, W.D., Gonzalez, A.L.C., Tang, F., Arballo, J.K., Okada, M., 1995a. Interplanetary origin of geomagnetic activity in the declining phase of the solar cycle. J. Geophys. Res. 100, 21717–21733.

Tsurutani, B.T., Gonzalez, W.D., Gonzalez, A.L.C., Tang, F., Arballo, J.K., Okada, M., 1995b. Interplanetary origin of geomagnetic activity in the declining phase of the solar cycle. J. Geophys. Res. 100, 21717–21733 A11.

Tsurutani, B.T., Gonzalez, W.D., 1997. The interplanetary causes of magnetic storms: a review. In: Tsurutani, B.T. et al., (Ed.), Magnetic Storms. Geophys. Monogr. Ser., 98, AGU, Washington, DC, pp. 77–89. https://doi.org/10.1029/GM098p0077.

Tsurutani, B.T., Gonzalez, W.D., Lakhina, G.S., Alex, S., 2003. The extreme magnetic storm of 1–2 September 1859. J. Geophys. Res. 108 (A7), 1268. https://doi.org/10.1029/2002JA009504.

Tsurutani, B.T., Gonzalez, W.D., Lakhina, G.S., Alex, S., 2005. Reply to comment by S.-I. Akasofu and Y. Kamide on “The extreme magnetic storm of 1–2 September 1859” J. Geophys. Res.. 110,https://doi.org/10.1029/2005JA011121 09227.

Tsurutani, B.T., et al., 2006. Corotating solar wind streams and recurrent geomagnetic activity: a review. J. Geophys. Res. 111, https://doi.org/10.1029/2005JA011273 A07S01.

Tsurutani, B.T., Verkhoglyadova, O.P., Mannucci, A.J., Saito, A., Araki, T., Yumoto, K., Tsuda, T., Abdu, M.A., Sobral, J.H.A., Gonzalez, W.D., McCreadie, H., Lakina, G.S., Vasyliunas, V.M., 2008. Prompt penetration electric fields(PPEFs) and their ionospheric effects during the great magnetic storm of 30–31 October 2003. J. Geophys. Res. 113. A05311, https://doi.org/10.1029/2007JA012879.

Tsurutani, B.T., Verkhoglyadova, O.P., Manucci, A.J., Lakhina, G.S., Huba, J.D., 2012. Extreme changes in the dayside ionosphere during a Carrington type magnetic storm. J. Space Weather Space Clim. 2, 05. https://doi.org/10.1051/swsc/20122004.

Tsurutani, B.T., Lakhina, G.S., 2014. An extreme coronal mass ejection and consequences for the magnetosphere and Earth. Geophys. Res. Lett. 41. https://doi.org/10.1002/2013GL058825.

Tsurutani, B.T., Echer, E., Shibata, K., Verkhoglyadova, O.P., Mannucci, A.J., Gonzalez, W.D., Kozyra, J.U., Pätzold, M., 2014. The interplanetary causes of geomagnetic activity during the 7–17 March 2012 interval: a CAWSES II overview. J. Space Weather Space Clim. 4, 02. https://doi.org/10.1051/swsc/2013056.

Tsurutani, B.T., Hajra, R., Echer, E., Gjerloev, J.W., 2015. Extremely intense (SML $\leq$ -2500 nT) substorms: isolated events that are externally triggered? Ann. Geophys. Commun. 33, 519–524. https://doi.org/10.5194/angeocom-33-519-2015.

Vasyliunas, V.M., 2011. The largest imaginable magnetic storm. J. Atmos. Sol. Terr. Phys. 73, 1444–1446. https://doi.org/10.1016/j.jastp.2010.05.012.

von Humboldt, A., 1808. Die vollständigsteallerbisherigenbeobachtungenüber den einfluss des nordlichts auf die magnetnadel. Ann. Phys. 29, 425–429.

Vichare, G., Alex, S., Lakhina, G.S., 2005. Some characteristics of intense geomagnetic storms and their energy budget. J. Geophys. Res. 110. A03204. https://doi.org/10.1029/2004JA010418.

Wang, C.B., Chao, J.K., Lin, C.-H., 2003. Influence of the solar wind dynamic pressure on the decay and injection of the ring current. J. Geophys. Res. 108 (A9), 1341. https://doi.org/10.1029/2003JA009851.

Willis, D.M., Stevens, P.R., Crothers, S.R., 1997. Statistics of the largest geomagnetic storms per solar cycle (1844–1993). Ann. Geophys. 15, 719–728.

Wu, J.-G., Lundstedt, H., 1996. Prediction of geomagnetic storms from solar wind data using Elman recurrent neural networks. Geophys. Res. Lett. 23, 319–322.

Wygant, J., Mozer, F., Temerin, M., Blake, J., Maynard, N., Singer, H., Smiddy, M., 1994. Large amplitude electric and magnetic field signatures in the inner magnetosphere during injection of 15 MeV electron drift echoes. Geophys. Res. Lett. 21, 1739–1742.

Yashiro, S., Gopalswamy, N., Michalek, G., St. Cyr, O.C., Plunkett, S.P., Rich, N.B., Howard, R.A., 2004. A catalog of white light coronal mass ejections observed by the SOHO spacecraft. J. Geophys. Res. 109. A07105. https://doi.org/10.1029/2003JA010282.

Yermolaev, Y.I., Nikolaeva, N.S., Lodkina, I.G., Yermolaev, M.Y., 2012. Geoeffectiveness and efficiency of CIR, sheath, and ICME in generation of magnetic storms. J. Geophys. Res. 117. https://doi.org/10.1029/2011JA017139 A00L07.

Yermolaev, Y.I., Lodkina, I.G., Nikolaeva, N.S., Yermolaev, M.Y., 2013. Occurrence rate of extreme magnetic storms. J. Geophys. Res. 118, 4760–4765. https://doi.org/10.1002/jgra.50467.

Yokoyama, N., Kamide, Y., 1997. Statistical nature of geomagneticstorms. J. Geophys. Res. 102, 14215.

FURTHER READING

Ji, E.-Y., Moon, Y.-J., Kim, K.-H., Lee, D.-H., 2010. Statistical comparison of interplanetary conditions causing intense geomagnetic storms (Dst ≤ -100 nT). J. Geophys. Res. 115. A10232. https://doi.org/10.1029/2009JA015112.

Kim, R.-S., Cho, K.-S., Kim, K.-H., Park, Y.-D., Moon, Y.-J., Yi, Y., Lee, J., Wang, H., Song, H., Dryer, M., 2008. CME earthward direction as an important geoeffectiveness indicator. Astrophys. J. 677, 1378.

Silbergleit, V.M., Zossi de Artigas, M.M., Manzano, J.R., 1996. Austral electrojet indices derived for the great storm of March 1989. Ann. Geofis. XXXIX (6), 1177–1184.

Tóth, G., Sokolov, I.V., Gombosi, T.I., Chesney, D.R., Clauer, C.R., Zeeuw, D.L., Hansen, K.C., Kane, K.J., Manchester, W.B., Oehmke, R.C., Powell, K.G., Ridley, A.J., Roussev, I.I., Stout, Q.F., Volberg, O., Wolf, R.A., Sazykin, S., Chan, A., Yu, B., Kóta, J., 2005. Space weather modeling framework: a new tool for the space science community. J. Geophys. Res. 110, A12226.

Tsurutani, B.T., Gonzalez, W.D., 1995. The efficiency of “viscous interaction” between the solar wind and the magnetosphere during intense northward IMF events. Geophys. Res. Lett. 22 (6), 663–666.

Tsurutani, B.T., Kamide, Y., Arballo, J.K., Gonzalez, W.D., Lepping, R.P., 1999. Interplanetary causes of great and super intense magnetic storms. Phys. Chem. Earth 24, 101–105.

Tsurutani, B.T., Verkhoglyadova, O.P., Mannucci, A.J., Araki, T., Sato, A., Tsuda, T., Yumoto, K., 2007. Oxygen ion uplift and satellite drag effects during the 30 October 2003 daytime superfountain event. Ann. Geophys. 25, 569–574.